OPEN

MedMat, Publish Ahead of Print

DOI: 10.1097/mm9.0000000000000050

Advancements in Hydrogel Microneedles for the Treatment of Myocardial Infarction

Jianxiang Li[a], Menghui Chen[a], Huipeng Wang[a], Jie Zhu[a] Hao Liu[a], Langqun Tan[a], Xiaoshun Yao[a], Le kang[a], Minyue Zhang[a], Chenggong Zhang[a], Xiaofeng Ding[c*], Yongxian Lai[c*], Dequn Wu[a, b*]

[a] *Key Laboratory of Textile Science and Technology, Ministry of Education, College of Textiles, Donghua University, Shanghai, 201620, China*

[b] *Innovation Center for Textile Science and Technology, Donghua University, Shanghai, 200051, China*

[c] *Department of Dermatologic Surgery, Shanghai Skin Disease Hospital, School of Medicine, Tongji-University, Shanghai, 200443, China*

[*] Corresponding author. *E-mail address*: dqwu@dhu.edu.cn

CRediT authorship contribution statement: Jianxiang Li: Investigation, Formal analysis, Writing - original draft. **Menghui Chen:** Data curation, Formal analysis. **Huipeng Wang:** Visualization. **Jie Zhu:** Data curation, Investigation. **Hao Liu:** Data curation. **Langqun Tan:** Data curation. **Xiaoshun Yao:** Validation. **Le kang:** Visualization. **Minyue Zhang:** Software. **Chenggong Zhang:** Methodology. **Xiaofeng Ding:** Resources. **Yongxian Lai:** Funding acquisition. **Dequn Wu:** Writing - review & editing.

Acknowledgments: This work was partially supported by the National Key Research and Development Program of China (project number: 2017YFB0309001) and the Natural Science Foundation of Shanghai (18ZR1400400, 18ZR1400500, 20ZR1402100).

Abstract:

Myocardial infarction (MI) remains a leading cause of morbidity and mortality worldwide, often progressing to heart failure due to inadequate tissue repair and adverse remodeling. Conventional therapeutic strategies, including pharmacological interventions and surgical procedures, exhibit limited efficacy in restoring cardiac function, highlighting the urgent need for innovative approaches. Hydrogel microneedles (MNs) have recently emerged as a groundbreaking technology for MI treatment, combining the advantages of minimally invasive delivery, targeted therapy, and multifunctional integration. Furthermore, the integration of therapeutic agents into hydrogel MNs enable sequentially controlled release within the infarcted myocardium, addressing key pathological processes such as oxidative stress, inflammation, and fibrosis. Additionally, the incorporation of conductive components into hydrogel MNs facilitate the restoration of electrical signal propagation, promoting synchronized cardiomyocyte contraction and mitigating arrhythmic. This article briefly surveys the latest advancements in hydrogel MN for cardiac repair. Key issues and challenges, as well as recommendations for future research, are also discussed.

Keywords: Myocardial infarction; Hydrogel microneedle; Minimally invasive delivery; Cardiac repair

1. Introduction

Cardiovascular diseases (CVDs) continue to represent the primary challenge faced by health systems around the world, accounting for significant proportion of worldwide mortality and morbidity [1]. In 2019 alone, CVDs are responsible for 11.86 million deaths globally, constituting an alarming 49.2% of total deaths [2,3]. It is anticipated that by 2030, the global economic burden of CVD is projected to reach $104.4 billion [4]. Within this extensive pathological conditions, myocardial infarction (MI), commonly known as a heart attack, is a significant and urgent expression of coronary artery disease [5,6]. Numerous risk factors relate to MI have been thoroughly examined, such as smoking, high blood pressure, abnormal lipid levels, diabetes, obesity, unhealthy eating habits, and a lack of physical activity [7]. Clinically, the primary mechanism of pathogenesis initiate with the rupture or erosion of a vulnerable atherosclerotic plaque within a coronary artery, setting off a series of events leading to intracoronary thrombosis that results in a sudden and significant blockage of blood flow. This ischemic insult leads to an irreversible necrotic demise of cardiomyocytes (CMs) within the territory supplied by the affected vessel, a process that began within mere minutes of oxygen deprivation [8]. The ensuing ischemic injury triggered a complex and multifaceted pathophysiological continuum. A swift and vigorous inflammatory response is activated to remove necrotic debris, which, if excessive and prolonged, paradoxically contributed to further tissue damage and inappropriate remodeling [9,10]. This remodeling is marked by progressive fibrosis, abnormal thinning of the ventricular wall, and harmful enlargement of the left ventricle, which ultimately affected cardiac output and increased the risk of heart failure.

Current treatments for MI, such as therapy and interventional surgery, are largely targeted at palliative care and have inadequately failed to tackle the fundamental problem of CMs loss,

especially during early MI [11,12]. Consequently, heart transplantation remained the only definitive treatment; however, this option is severely limited by an inadequate supply of donor organs, which consistently fails to keep pace with the growing patient demand. Despite paradigm-shifting advances in acute reperfusion therapy, including percutaneous coronary intervention (PCI) and thrombolysis that successfully salvage the ischemic myocardium, these interventions are fundamentally and temporally limited to the acute phase of the disease [13]. They ultimately fail to effectively tackle the several waves of inflammation, cell death, and fibrotic scarring that subsequently and persistently characterize the environment post-MI [14]. Consequently, a truly significant therapeutic deficit persistently remains, which fundamentally necessitates that future strategies extend beyond merely halting maladaptive processes to proactively and robustly reversing them, thereby directly facilitating truly substantial cardiac repair and regeneration.

Hydrogel microneedles (MNs) have increasingly emerged as a revolutionary technological paradigm, seamlessly integrating minimally invasive deployment precision with multifaceted therapeutic functionality. This sophisticate approach enabled direct trans myocardial access while entirely circumventing the procedural complexities associated with invasive surgical interventions. The particularly unique architectural configuration of MN arrays reliably permitted robust epicardial adhesion, consequently establishing an intimate biointerface for sustained therapeutic release exclusively within the compromised myocardial region. Furthermore, the inherent modularity of hydrogel MNs facilitate the incorporation of diverse bioactive payloads, while simultaneously permitting the integration of conductive materials to address the critical electrophysiological desynchrony that followed ischemic injury. In this review, the interaction between hydrogel MNs and myocardial repair post-MI will be

comprehensively explored (Figure 1). The pathological microenvironment post MI, the design principles and fabrication methodologies of hydrogel MNs, as well as the current status, challenges, and prospects of functional hydrogel MNs for repairing damaged myocardial tissue systematically are proposed. This review seeks to clarify the trajectory of hydrogel MNs as a hopeful new frontier in the continuous endeavor for significant myocardial repair and functional recovery.

2. Pathological Post MI

MI is frequently associated with severe systemic or structural heart disorders, such as hypertension, valvular heart disease, and coronary artery stenosis or obstruction [7,15]. The progressive pathological alterations that occur post-MI exhibits high complexity, posing significant challenges for clinical intervention [16]. Owing to impaired myocardial self-repair capacity and insufficient regenerative potential, MI ultimately progresses to heart failure (HF), accompanied by neurohumoral overactivation, excessive inflammatory responses, and chronic cardiac remodeling [17]. The pathophysiological progression from MI to HF could be categorized into four distinct yet temporally overlapping phases (Figure 2): the early acute injury phase, inflammatory response phase, tissue proliferation and repair phase, and adverse remodeling phase. Understanding insight into the specific pathophysiological mechanisms underlying each phase could guide the definition of therapeutic targets and the development of corresponding treatment strategies.

2.1. Early acute injury

During the early phases of MI, the obstruction of coronary arteries lead to a detrimental reduction of blood supply, causing localized ischemia and hypoxia [18]. This compromised microenvironment significantly affects the function of the high density mitochondria found

within CMs, which in turn disrupts the normal metabolism of ATP [19]. Consequently, there is an abnormal increase in the levels of reactive oxygen species (ROS), which contribute to the development of myocardial ischemia/reperfusion injury [20]. The dysfunction of mitochondrial processes further exacerbated the situation by redirecting cellular energy production from aerobic respiration to anaerobic glycolysis. Consequently, this shift promotes the accumulation of various metabolic byproducts, such as lactate, within the affected tissue. As these metabolites build up, they contribute to a decline in the local pH, creating an even more hostile environment for the cardiac cells [21,22]. Elevated levels of ROS play a critical role in triggering the overproduction of inflammatory cytokines, which, in turn, initiate a severe inflammatory response within the affected tissues. This heightened inflammatory environment not only contribute to cellular damage but also increase the permeability of the mitochondrial permeability transition pore. As a result, there is a significant exacerbation in the loss of cytochrome c, a crucial component in the mitochondrial apoptosis pathway [23]. This pathological sequence of events ultimately leads to the necrosis and programmed cell death of CMs, further compounding the damage to cardiac tissue. The abrupt decline in the number of viable CMs have serious repercussions for cardiac structure and function. Specifically, the reduction in CMs results in thinning of the ventricular wall, which elevate mechanical stress on the heart. Such structural changes can precipitate complications such as chamber dilation or the formation of ventricular aneurysms [24]. These alterations significantly heighten the risk of cardiac rupture, a potentially fatal condition. Additionally, the loss of myocardial viability in the infarcted region disrupts the normal hemodynamics of the heart, further compromising its functionality and overall capacity to pump blood effectively. Non-infected regions exhibit functional hyperactivity, which triggers neurohormonal regulation. This includes the excitation of the

sympathetic adrenaline system, activation of the renin-angiotensin-aldosterone system, and secretion of natriuretic peptides (ANP [atrial natriuretic peptide] and BNP [B-type natriuretic peptide]) aim at stabilizing cardiac output and facilitating transient circulatory compensation. However, this early compensation stabilization is considered symptomatic. The precocious activation of neurohormonal regulation initiate the malignant cycle associated with long-term adverse ventricular remodeling. At this stage, it is imperative to proactively implement reperfusion therapies to prevent further enlargement of the MI region. Concurrently, excess ROS must be cleared, and mitochondrial functionality should be enhanced to mitigate ischemia/reperfusion injuries resulting from blood perfusion.

2.2. Inflammatory response

Necrotic tissue and ECM degradation initiate a cascade of sterile inflammation, which involve intricate molecular and cellular events [25,26]. Initially, neutrophils move in, while monocytes are drawn from the bloodstream and travel to the infarcted region, where they transform into macrophages to perform phagocytosis [27]. Simultaneously, macrophages release growth factors such as VEGF and basic fibroblast growth factor, which promote neovascularization and thereby foster a more conducive microenvironment [28]. At this stage, macrophages predominantly display an M1 proinflammatory phenotype. This particular phenotype plays a crucial role in initiating and sustaining local inflammatory processes. By releasing various cytokines, these M1 macrophages contribute to the recruitment of additional immune cells to the site of injury or infection, thereby driving direct inflammation. While inflammation is often perceived negatively, it is important to recognize that an appropriate inflammatory response is essential for subsequent tissue repair and healing, facilitating the recovery process in the affected area. However, excessive or protracted inflammation can inflict

further damage upon the surviving myocardium and adjacent healthy tissue [29,30]. Hence, a key therapeutic objective of hydrogel MNs therapy is to modulate the inflammatory response and promote angiogenesis through the localized delivery of bioactive agents.

2.3. Tissue proliferation and repair

This decisive phase, which determine the potential progression to heart failure, is marked by abundant local TGF-β1 production from necrotic CMs and macrophages, inducing fibroblast chemotaxis [31] . The reparative collagen fibers undergo weeks of cross-linking, maturation, and aging to form a stable scar. This maturation culminate in a structure that, despite providing critical mechanical support and stress distribution, remains electromechanically inert and non-contractile compared to the healthy heart muscle [32]. Under physiological conditions, myofibroblasts undergo programmed apoptosis to prevent excessive fibrosis [33]. In the infarcted heart, however, this regulatory process is often overwhelmed by a marked upregulation of matrix metalloproteinases (MMP-2 and MMP-9), which derive adverse ventricular remodeling by degrading the ECM [34]. Therefore, therapeutic strategies for this phase are designed to orchestrate a transition in macrophage polarization from the M1 to the M2 phenotype, resolve inflammation, inhibits MMP activity, and ensure balanced collagen deposition.

2.4. Adverse remodeling

Persistent activation of myofibroblasts and subsequent overproduction of collagen could occur when the scar tissue fails to compensate for the sustained mechanical stress and deformation of the ventricular wall [35]. Initially, collagen deposition confine to the infarcted region, however excessive collagen deposition often extends beyond the infarct into the peri-infarct and remote myocardium, thereby increasing tissue stiffness [36]. These mature fibrotic scars form an electromechanically isolated region, which disrupts synchronous cardiac

contraction and create an arrhythmogenic substrate, ultimately manifesting as pump failure and conduction anomalies[37]. To compensate for localized cardiac dysfunction, the body engage neurohumoral regulatory mechanisms. However, sustained activation of these responses increase the mechanical load on the heart, which in turn exacerbate peri-infarct fibrosis and induces myocardial hypertrophy [38]. These changes further impair cardiac function and paradoxically amplify neurohumoral activation. This establishes a self-perpetuating cycle driven by mismatched mechanical stress, electrical desynchrony, and excessive neurohumoral signaling, ultimately leading to progressive ventricular remodeling and HF. Overcoming the limitations of current therapies remains a major hurdle in MI treatment, creating a pressing demand for more cost-effective therapeutic solutions.

Table 1 provides a systematic mapping between post MI pathological stages and the corresponding design strategies of hydrogel MNs for cardiac repair. The table categorizes the post-MI progression into four sequential phases: acute injury (0-24 h), inflammatory phase (1-7 d), proliferative/repair phase (7-21 d), and remodeling/scar formation phase (>21 d). For each phase, the key pathological features ranging from ROS burst and cardiomyocyte necrosis in the acute stage to fibrosis and ventricular wall thinning in the chronic stage are explicitly linked to targeted hydrogel MN functionalities, including ROS scavenging, immunomodulation, pro-angiogenesis, and anti-fibrotic mechanical support. Representative therapeutic agents for each stage, such as antioxidants, anti-inflammatory cytokines, growth factors (VEGF, bFGF), exosomes, and anti-fibrotic drugs, are also summarized. This stage directed framework offers readers a clear roadmap for rational design of hydrogel MNs tailored to specific post-MI pathophysiological needs.

3. Classification of Cardiac Patches

Current research on cardiac patches for MI treatment primarily focuses on four promising types: fibrous films [39,40], elastomer [41,42], hydrogels [43,44] and hydrogel MNs [45-47]. Fibrous films, typically fabricate from polymers including polycaprolactone, polyurethane, and gelatin via electrospinning, are commonly sectioned into specific dimensions from electrospun mats. These nanofibrous films exhibits inherent elasticity and could be further functionalized to improve conductivity [48,49], enhance bioactivity, and achieve controlled therapeutic release through techniques such as grafting and layer-by-layer assembly [50]. Elastomers, derived from materials like poly(glycerol sebacate) (PGS) and polyurethane, are recognized for their remarkable elasticity and deformability [51,52]. Recent studies integrate such elastomeric patches with complementary strategies to develop comprehensive therapeutic systems [53]. The hydrogel, which constitutes the most prevalent category, is primarily fabricated from biocompatible materials such as decellularized ECM (dECM), collagen, alginate, and poly(ethylene glycol). These material exhibits excellent biocompatibility, tunable mechanical properties, and a porous microstructure, which allows for the encapsulation of cells, active factors, or conductive materials to achieve diverse therapeutic goals [54]. Lastly, MN patches feature dense arrays of micron-scale needles (height: 10–2000 μm; width: 10–50 μm) that are fabricated via molding or 3D printing from materials such as poly(vinyl alcohol) (PVA), hyaluronic acid (HA), and gelatin methacryloyl (GelMA) [22,55]. The greater thickness of the ventricular wall in large animals and humans renders simple epicardial permeation ineffective, especially for deep myocardial infarcts [56]. To overcome this limitation, hydrogel MNs overcome this barrier by using penetrating tips to create micro-channels between the MNs and the heart tissue, thereby enabling accurate and targeted delivery of cells, regenerative factors, or pharmacological agents to deep regions [57-60].

In contrast to intramyocardial injections, the microscale tips of microneedles markedly lower the potential for cardiac structural damage. This structural benefit, combined with their capabilities in minimal invasiveness, flexible drug loading, controlled release, and tissue integration, establishes hydrogel MNs as a multifunctional platform with composite advantages over other delivery systems.

Table 2 compares hydrogel MNs with existing cardiac drug delivery strategies. Intramyocardial injection, although clinically established, is limited by rapid drug washout due to cardiac motion and uneven distribution resulting from a single bolus. Conventional hydrogel patches offer sustained release but rely on passive diffusion, which restricts penetration into the myocardial wall. Nanoparticle-based delivery systems enable targeted delivery and prolonged circulation; however, cardiac accumulation remains inefficient, and systemic off target effects pose ongoing concerns. Hydrogel MNs uniquely combine mechanical anchoring, tunable release kinetics, and direct parenchymal penetration. Nevertheless, they are not without limitations: fabrication is more complex, drug loading capacity per needle is relatively low, and the long-term presence of penetrating foreign bodies raises safety questions regarding arrhythmogenicity and chronic inflammation. Therefore, hydrogel MNs are best viewed as a complementary tool, particularly valuable for delivering biologics or bioactive molecules that require both sustained release and precise spatial distribution within the infarct border zone, rather than a universal replacement for existing methods.

4. Hydrogel MNs

Microneedle technology sees significant progress since its inception with a solid device patent in 1971 [61], marked by a transition from basic metal poke and patch systems to advanced, controllably swelling polymeric MNs [62]. Conventional MNs, including solid, hollow, coated,

and dissolving types, are widely documented [63] (Figure 3A). A notable milestone occurs in 2012 with the introduction of hydrogel MNs [64], which represents a significant evolution in the field. This technology uniquely combines the physical penetration of microneedle arrays with the versatile biological functionality of hydrogels (Figure 3B), establishing adaptable and effective platform. Furthermore, hydrogel MNs function by penetrating the stratum corneum to absorb interstitial fluid (ISF), a process central to their application in biomarker sensing [65,66]. Their gelation, achievable through physical, electrostatic, or covalent cross-linking, allows for a range of preparation methods contingent on the selected materials and cross-linking chemistry.

4.1. Design hydrogel MNs

The design of microneedle (MN) arrays is application driven, leading to a wide variety of geometries. When designing MNs, particularly hydrogel-based systems, several parameters are crucial. A key consideration is balancing the array configuration and needle dimensions with the swelling capacity of material to ensure optimal performance; a summary of these design parameters is provided in Table 3.

The needle length, designated as *L* in Figure 3C, is a critical design parameter, which must be carefully optimized. As pain-sensing nerve endings are concentrated in the dermis, increased needle length raises the probability of activating these receptors during insertion. This provokes pain and discomfort, which in turn may hinder the clinical acceptance and widespread adoption of MN technology. Gill et al. [67] investigate the relationship between MN length and application pain, which pain scores increase from 5% to 37% as length grew from 480 μm to 1450 μm—corresponding to a sevenfold increase, with 100% defined as the pain from a standard hypodermic needle. The mechanical strength of hydrogel MNs is inversely related to needle length, posing a risk of structural damage with longer designs [68]. To concurrently ensure

sufficient skin penetration (requiring lengths above the typical minimum, see Table 3) and maintain structural integrity, researchers predominantly fabricate hydrogel MNs with lengths ranging from 500 to 800 μm.

The base width of MNs, denoted as D_b is a key geometric parameter governing mechanical strength (Figure 3C), with wider bases reducing needle fragility [67]. Critically, the enhancement in robustness comes without the trade-off of increased patient discomfort, as width shows no correlation with pain [67]. Optimizing inter-needle spacing is crucial, as overly narrow spacing distributes the insertion force (the "bed of nails" effect), potentially preventing full penetration [69]. Conversely, for hydrogel MNs, such spacing also accommodates needle swelling to avoid inter-needle collision and array damage.

As a key design parameter, the tip diameter (D_t, Figure 3C) directly determines the penetration force. The sharper tips (D_t < 15 μm) significantly reduce insertion force and ensure smooth skin penetration, thereby optimizing overall application efficacy [70]. The decisive role of tip geometry is highlighted by Römgens et al., who recorded that the force required for skin penetration rises from 20 mN per MN for a 5 μm tip radius to 167 mN for a 37 μm radius [70]. Complementing tip sharpness, the overall needle shape is equally vital for easy insertion [67]. The conical shape is traditionally dominant, though pyramidal designs are now gaining prominence [71]. The prevalence of conical and pyramidal shapes is attributed to their excellent mechanical performance during insertion [68]. Alternative shapes have been investigated but present significant challenges in fabrication, reliable skin penetration, or clean extraction [62]. Beyond individual needle dimensions, the array size ($A_x \times A_y$, Figure 3C) is another critical parameter. To mitigate the "bed of nails" effect, researchers often employ smaller arrays with lower needle density. Despite the widespread use of low-density arrays, Ramöller et al. [72] demonstrate the

viability of high-density designs. The groups report that at an application force of 32 N, penetration efficiency is comparable between low-density (220 needles·cm^{-2}) and high-density (800 needles·cm^{-2}) arrays. However, the high-density configuration enables a greater volume of drug release or ISF extraction.

It is important to distinguish MN systems designed for transdermal applications from those intended for cardiac tissue. While transdermal MNs focus on painless skin penetration, nerve avoidance, and sustained drug release into the dermis, cardiac MNs operate in a fundamentally different environment. The myocardium undergoes continuous contraction and relaxation, lacks sensory nerve endings, and requires robust yet atraumatic anchoring. Furthermore, cardiac MNs must avoid coronary vessels, penetrate only the infarct or border zone without reaching the ventricular lumen, and degrade over weeks to months to align with the post MI remodeling process. Consequently, design parameters optimized for the skin, such as needle length for avoiding nerve plexuses or force thresholds for painless insertion, lose their direct relevance when applied to the heart. Instead, cardiac MN enabled patches prioritize dynamic conformability, anti-arrhythmic safety, and seamless integration with the mechanical cycle of the beating heart.

4.2. Fabrication of hydrogel MNs

4.2.1. Micro-molding

The predominant and most recognized technique for manufacturing hydrogel MNs is micro-molding [76]. This method encompasses several approaches, including laser drilling, injection molding, and the casting of polymer materials, all of which are employed to create a micro-mold [72]. By utilizing these various techniques, researchers are able to develop precise and effective microneedle designs that are essential for applications in MI fields. This technique is frequently

employed because the micro-molds can be reused and are capable of producing several hydrogel MN arrays simultaneously [82]. Additionally, micro-molding facilitates rapid and straightforward fabrication of hydrogel MNs, which is particularly advantageous during parameter optimization [83]. The prevalent method of micro-molding typically involves the casting of polymers, specifically utilizing poly(dimethylsiloxane) (PDMS). This material is arranged around a solid master template of MNs and is cured for 2 h at a temperature of 70 °C. Once cured, the master template could be extracted, resulting in a negative micro-mold that can be employed for the creation of hydrogel MNs (Figure 3D) [84]. A key distinction within the polymer casting micro-molding technique lies in the process used to fabricate the solid MN master template.

4.2.2. 3D printing

3D printing technologies, particularly photopolymerization-based techniques such as digital light processing and stereolithography, enable a revolutionary one-step molding strategy for fabricating hydrogel MNs [85]. This approach employs computer aided design models to program ultraviolet light patterns, which selectively polymerize hydrogel prepolymers, loaded with bioactive molecules, in a layer-by-layer or projection-based manner. Consequently, it allows the direct and precise fabrication of hydrogel MN arrays with complex macrostructures and micro-scale surface topographies, eliminating the need for traditional molding processes. Compared to conventional molding, this method circumvents the need for physical molds, accelerating development and enabling unprecedented customization in microneedle design. It allows for precise control over all geometric parameters (shape, height, density) and, through multi-material printing, can create heterogeneous structures for spatiotemporal drug release. For instance, distinct drugs can be compartmentalized within the tip and base of a single needle, offering a flexible platform for sophisticated transdermal delivery.

While both micro-molding and 3D printing have enabled the development of proof-of-concept cardiac MN patches, their translational feasibility differs substantially. Micro-molding offers clear advantages in scalability, batch to batch reproducibility, and cost per unit at production scale, positioning it as the preferred route for mass produced, off the shelf patches. However, this approach requires high initial investment in master mold fabrication and offers limited adaptability to patient specific geometries. In contrast, 3D printing provides unparalleled design flexibility, enabling rapid iteration of needle geometry, spatial heterogeneity, and even patient specific patches tailored to infarct topography. Nevertheless, current 3D printing technologies face significant barriers to clinical translation, including low throughput, high per-unit cost, batch variability, and unresolved challenges related to sterilization and residual monomer toxicity. These comparative parameters are summarized in Table 4. From a translational perspective, micro-molding is likely to lead near term clinical adoption, whereas 3D printing may find its niche in personalized or point of care manufacturing once regulatory pathways for additively manufactured medical devices mature.

4.3. Clinical Translation Perspective

To fully appreciate the translational potential of hydrogel MNs, it is essential to compare them with both current standard of care and emerging therapies for MI. Intravenous injection, the most common route of drug administration, is limited by low cardiac retention and significant off target toxicity. Intracoronary infusion offers only a modest improvement in cardiac retention, yet it requires specialized facilities and provides only transient therapeutic exposure. Epicardial cardiac patches enable localized drug delivery but necessitate open chest surgery and carry risks of constrictive pericarditis and adhesion formation. Drug eluting stents effectively address epicardial vessel stenosis but do not target the myocardial interstitium. In contrast, hydrogel

MNs occupy a unique therapeutic niche by enabling site specific delivery directly to the infarct border zone, providing sustained release of therapeutics over days to weeks, allowing minimally invasive deployment potentially via catheter-based systems, and offering mechanobiological support through mimicking the native cardiac extracellular matrix.

In response to the four major bottlenecks currently limiting the clinical adoption of hydrogel MNs, specific solutions are proposed based on existing literature and insights (Table 5). First, to address delivery precision under dynamic conditions, solutions include integrating real-time imaging, developing shape-memory or magnetically steerable MNs deployable via catheters, and employing soft robotics to compensate for cardiac motion. Second, for scalability and GMP manufacturing, recommended approaches include continuous manufacturing technologies, pre-sterilized GMP-grade raw materials, quality-by-design frameworks, and industry-academic consortia to standardize characterization protocols. Third, regarding long-term safety and degradation product fate, proposed strategies involve designing biodegradable hydrogels with benign, renally clearable byproducts, conducting ≥6-month large-animal studies with comprehensive histopathology, cardiac electrophysiology, and biodistribution analyses, and incorporating biodegradation modeling to predict in vivo behavior. Fourth, to resolve regulatory pathway ambiguity, a stepwise de-risking framework is suggested: (Step 1) establish material safety and biocompatibility per ISO 10993; (Step 2) generate GMP-compliant pilot batches with full characterization; (Step 3) conduct pivotal large-animal efficacy and safety studies using clinically relevant delivery; and (Step 4) engage regulatory agencies early via pre-submission meetings (FDA Pre-Submission Program). Publication of negative data on failed translational attempts is also encouraged to inform regulatory science. Overall, the field must shift from proof-of-concept studies toward solving delivery precision and scalable GMP manufacturing, as

these are the true rate-limiting steps for clinical adoption. Long-term safety and regulatory clarity, while challenging, can be addressed in parallel through well-designed large-animal studies and early agency engagement. By confronting these limitations head-on with actionable solutions, the translational promise of hydrogel MNs for cardiac repair can be realized.

5. Material Selection

Hydrogel MNs are fabricated from a diverse range of synthetic, natural, and conductive materials, allowing their properties to be tailored for specific therapeutic applications by adjusting material combinations and ratios. The advantages, disadvantages, and general characteristics of these materials are summarized in Table 6.

5.1. Synthetic materials

Synthetic materials are extensively used in hydrogel MN due to their controllable sources, excellent mechanical properties, and low immunogenicity. Notable examples include polyetherimide [87], polyurethane [88], poly-ε-caprolactone [89,90], poly(ethylene glycol) [91,92], carboxymethyl cellulose [93], poly(N-isopropylacrylamide) [94], and poly(lactic-co-glycolic acid) [95], PVA. The PVA is especially prominent for its high hydrophilicity and biocompatibility in patch fabrication. Fan et al. [96] design a micro-needle patch loaded with VEGF and near-infrared (NIR)-light-triggered self-unfolding graphene oxide-PVA for minimally invasive surgery treatment of MI. Leveraging shape memory effects, the patch can be implanted into the thoracic cavity via a 4 mm incision. Following 10 s of NIR irradiation, it rapidly restores its original shape and anchors itself to the cardiac surface. This enables controlled release of VEGF, promote angiogenesis, reduce myocardial fibrosis, and restore cardiac function (Figure 4A). Synthetic materials are characterized by their tunable mechanical properties and excellent processability. These inherent properties enable MNs made from synthetic materials to provide immediate

mechanical support and function effectively without the need for cellular or other active components.

5.2. Natural Materials

Natural materials, sourced from environmental polymers like proteins (fibrin, collagen [97,98], gelatin), polysaccharides (HA, chitosan [99,100], alginates [101,102]), and dECM, preserve innate biological structures. Consequently, these materials inherently retain their natural structure and biological characteristics, offering excellent biocompatibility while promoting cell adhesion and proliferation. While fibrin patches can directly ameliorate cardiac function post-MI, they are typically employed as cellular carriers owing to a shortage of inherent bioactivity [103,104]. Gelatin, produced from collagen hydrolysis, is often chemically functionalized (gelatin methacryloyl) for cardiac MN patch applications [105,106]. Chen et al. [107] fabricate a galunisertib-loaded MN patch from GelMA using a molding technique. The MN path exhibit the mechanical strength of up to 0.4 $N \cdot needle^{-1}$, which is sufficient to penetrate myocardial tissue without fracture. The MN patch provide a sustained release of galunisertib over 15 d, which effectively inhibit the transforming growth factor-β (TGF-β)/Smad2 signaling pathway, thereby controlled fibroblast differentiation and reduce collagen deposition. Additionally, Liu et al. [46] develop a biodegradable HA MN patch (CRO-DMN), utilizing the natural polysaccharide structure of HA, which consist of repeating glucuronic acid and N-acetylglucosamine units [108]. The CRO-DMN patch penetrate the stratum corneum to release drugs within 30 min and support skin healing within 90 min. In a mouse MI model, it significantly improves cardiac function, diminish infarct size, exert protective effects on myocardial tissue and mitochondria, and enhance vascular regeneration (Figure 4B). The dECM patches, which are rich in growth factors and matricellular proteins, facilitate cardiac repair and angiogenesis via bio-inductive mechanisms and have

received clinical approval for MI repair [37,109]. Although natural materials like dECM are excellent bioactive carriers, their translation is hampered by batch heterogeneity originating from biological variability and the demanding storage conditions required for stability, necessitating further development for widespread clinical use.

5.3. Conductive materials

Native cardiac tissue exhibit the conductivity of approximately 1.5-1.7 × 10^{-3} S·cm^{-1} [110], whereas necrotic and scar tissue are non-conductive. Conductive hydrogel MNs possessing conductivities comparable to or greater than native myocardium can be applied via electrocoupling (Figure 4C). This approach reestablishes electrical conduction, reduce arrhythmic risks, and prevent the adverse ventricular remodeling caused by chronic conduction heterogeneity. Common conductive materials for hydrogel MNs encompasses conductive polymers (polypyrene, polyaniline [111,112], PEDOT [113,114]), carbon-based nanomaterials (e.g., carbon nanotubes [115,116], graphene oxide [12,96]), and others such as nanogold [39,117], ionic compounds [118,119] and MXene. Although polypyrene provide advantages such as biocompatibility and straightforward processing [120], conductive polymers often clump together in water solutions because of their hydrophobic nature, which negatively impact conductivity. Consequently, approaches such as catechol functionalization are employed to obtain a uniform distribution within hydrogel MNs. Mao et al. [55] synthesize the conductive hydrogel termed GelMA-PPy-PDA by modifying GelMA with polypyrrole and dopamine. The hydrogel is then used to encapsulate LaRG@ZIF-90-TPP nanoparticles, forming a conductive microneedle patch (designated as MN-PPy-PDA). During fabrication, a negative mold with ordered conical microcavities is utilized to ensure the precise alignment of the microneedles within the patch (Figure 4D). MXene, a graphene-like 2D conductive material first reported in 2011 [121], exhibit

excellent conductivity, hydrophilicity, and dispersion stability due to its surface functional groups (-OH, -F). Its integration into natural polymers such as gelatin has enabled the development of conductive hydrogel MN patches with high conductivity (18.3×10^{-3} S·cm^{-1}) and cardiac tissue-like elasticity (30.4 kPa) [122]. These Ti_3C_2 MXene nanosheets also function as effective ROS scavengers to mitigate oxidative injury [123]. Nevertheless, as most inorganic conductors are non-degradable and rely on excretion for clearance, their potential long-term toxicity due to bio-accumulation required thorough safety investigation. The mechanical strain and deformation of the ventricles during cardiac cycles induce corresponding resistance changes in conductive hydrogel MN patches. Recent studies have capitalized on this phenomenon to convert mechanical activity into electrical signals, allowing for the real-time tracking of diastolic-systolic amplitude, heart rate, and rhythm (Figure 4E) [43,111]. Consequently, the combination of real-time monitoring with therapeutic electrocoupling in a single device emerges as a promising strategy for advancing the functionality of conductive cardiac patches.

6. Optimal Properties for Hydrogel MNs

The definition of the properties of hydrogel MN material, which include mechanical performance, biocompatibility, degradability, and conductivity is essential during the design and development of hydrogel MNs. Considerations associated with cost, sourcing constraints, large-scale producibility, and storage demands have become equally vital as advancement proceeds toward the phase of clinical implementation.

6.1. Mechanical properties

To withstand the dynamic stresses of the beating heart, hydrogel MNs require a combination of mechanical properties, including high elongation at break, toughness, flexibility, and fatigue resistance to prevent failure. Furthermore, while optimal stiffness is crucial for

mechanical integration and ventricular support, excessive stiffness could impair cardiac output, leading to adverse ventricular remodeling and diastolic dysfunction. According to the Law of Laplace, sustained left ventricular restraint therapy for MI act by reducing ventricular stress and dilation to curb remodeling and conserve function, necessitating that the hydrogel MN embody suitable stiffness, toughness, and flexibility. Although native cardiac tissue exhibit the Young's modulus of 10-15 kPa [124], the optimal modulus for the hydrogel MNs, defined as the slope of the elastic region, is suggested to be a much wider range, from tens of kPa to MPa [125,126], with actual myocardial stiffness being variable across species, age, sex, and pathology. Ischemia-induced myocardial fibrosis, for instance, elevate ventricular wall stiffness to 30-50 kPa [127]. The limited success of purely mechanical approaches is highlighted by the Acorn trial over a decade ago, which find that ventricular restraint offer only symptomatic relief and did not effectively prevent progression to end-stage heart failure [128] or improve mortality [129]. This underscore that the failure likely stem from a rudimentary understanding of the underlying physiological mechanisms and the challenge of matching a static implant to the pathologically dynamic stiffness of the remodeling heart. To address the persistent morphological changes of heart, Wang et al. [22] design a PLGA needle/substrate assembly. The measured single-needle strength is highest at ~0.7 N, in contrast to the PLGA/ESMP needle-effervescent substrate, which is the weakest at 0.5 N. Unlike conventional hydrogel, this novel hydrogel MNs exhibit distinct mechanical and rheological properties under the stress of cardiac contractions. This unique design allows it to autonomously adapt to the periodic deformation of myocardial tissue, providing sustained support that alleviated ventricular dilation and effectively counteracts the decline in cardiac output.

6.2. Biocompatibility and degradability

Biocompatibility serves as a fundamental prerequisite for the successfully clinical translation of the hydrogel MNs and their degradation products. The implantation of the hydrogel MN result in a negligible foreign-body response, effectively mitigating the risks of severe inflammation, excessive ECM deposition, fibrosis, and tissue adhesion. Furthermore, the hydrogel MNs demonstrate low systemic toxicity to prevent potential damage to vital organs, including the liver and kidneys [130]. To meet optimal biocompatibility standards, an implanted hydrogel MN should cause little to no acute inflammation that resolved over time, while preserving hepatic and renal function. Therefore, thorough evaluation is critical, entailing the analysis of immune responses [131], longitudinal monitoring of inflammation (especially in large animals), and measurement of relevant clinical biochemistry markers, including liver enzymes (ALT, AST), albumin/globulin ratio, and renal function indicators (BUN, creatinine). Although autologous materials derive from the patient themselves help mitigate immune rejection, the degradation profile of hydrogel MNs must be adapted to the individual's clinical status and disease progression. Those with advanced heart failure or contraindications for major interventions require persistent mechanical support; here, non-degradable polymers are preferable to maintain long-term structural and functional stability. While degradable MNs provide temporary mechanical support and localized drug delivery, their degradation rate must be carefully tuned. Excessively rapid breakdown, as in some dECM-based MNs, risks premature failure, whereas overly slow resorption can necessitate removal. By developing composite materials, researchers have prolonged mechanical support and achieved synchronized, controlled release of bioactive, thus optimizing treatment duration.

7. Hydrogel Microneedles for MI

7.1. Smart responsive

Post MI, the extracellular pH dropped rapidly from 7.4 to as low as 5.9 [22], thereby influencing a variety of ion channels. Concurrently, the intracellular pH also decrease due to the accumulation of hydrogen ions (H^+) and lactate ions within cells [132]. In the early of ischemia, the development of acidosis may act as a regulatory mechanism that reduces contractility and ATP consumption, thereby helping to preserve cellular integrity [133]. In response to the complex pathological microenvironment that arise post MI, a smart hydrogel MNs patch utilizing a dual-response mechanism to react to ROS and pH levels present a promising strategy for targeted cardiac repair [134-136]. The hydrogel MNs is designed to sense and respond of the infarcted heart: high levels of ROS (e.g., H_2O_2) from ischemia-reperfusion injury and an acidic microenvironment resulting from anaerobic metabolism. Yang et al. [10] develop a pH and ROS dual responsive smart injectable hydrogel loaded with C-type natriuretic peptide (CNP) and Semaphorin 3A for MI treatment (Figure 5A). Moreover, this dual-response mechanism ensures precise spatiotemporal drug delivery to the most critical infarct areas, effectively scavenging excess ROS to alleviate oxidative stress, modulated inflammatory responses as well as promote angiogenesis and myocardial tissue repair. Although responsive hydrogel MNs remain still in the early phase of being directly applied to MI research, with relatively limited studies to date. Nevertheless, their distinctive "intelligent" responsiveness presents significant potential for tackling numerous critical issues in the repair of infarctions. For instance, by designing MNs that respond to specific enzymes overproduce in the infarct region, targeted and on-demand drug delivery at the lesion site can be achieved. This approach allows for precise management of

inflammation, suppression of fibrosis, and stimulation of angiogenesis, providing a groundbreaking alternative to traditional drug delivery techniques.

7.2. Monitoring and treatment

Hydrogel MNs represent a frontier technology in transdermal drug delivery and biosensing, evolving from simple mechanical perforators to sophisticated theragnostic platforms [137]. By integrating stimuli-responsive hydrogels as the matrix, these MNs achieve synergistic monitoring and treatment capabilities, paving the way for closed-loop biomedical systems. The operational paradigm typically involves the penetration of hydrogel MN array into the superficial dermis, allowing the MNs to extract ISF biomarkers and respond to specific pathological cues. Yang et al. [138] develop a wearable dual-mode patch, referred to as the e-SERS patch, which integrate surface-enhanced Raman scattering (SERS) microneedle arrays with flexible electronics for the rapid pre-hospital diagnosis of MI. Furthermore, the patch facilitates non-invasive and rapid monitoring of three myocardial injury markers in electrocardiograms (ECG) and ISF using a portable Raman spectrometer. Finally, the patch significantly reduces the time to ischemia diagnosis to just 50 min post-onset, as validate in rat MI models (Figure 5B). Similarly, Zhang et al. [139] develop a wearable system for dynamic MI monitoring, which integrate strain-insensitive and self-adhesive SCL bioelectrodes, the flexible ECG patch, and the machine learning-based algorithm for MI identification and localization. The SCL electrode, compose of styrene-isoprene-styrene, carbon nanotubes, and liquid metal, exhibit exceptional stability with minimal resistance variation under 100% strain and an adhesive strength exceeding 0.4 $N \cdot cm^{-1}$. This integrated system enables continuous, synchronous multi-lead ECG acquisition and, when combine with the machine learning model, achieve remarkable MI identification accuracy of 99.93%. Furthermore, the system incorporates an automated annotation framework for abnormal

signal segments, thereby supporting personalize early warning and intervention strategies for MI (Figure 5C). Furthermore, Yu et al. [111] have developed a time-dependent adhesive hydrogel patch that enables real-time monitoring of micro-deformations in the diastolic-systolic mechanical physiology of MI. This innovative approach, through electrically couple therapy, inhibit ventricular remodeling, promote vascular regeneration, and enhance electro-cardiological function. Consequently, the adhesive hydrogel patch offers an integrated diagnostic and therapeutic solution for MI, facilitating continuous monitoring. This sense-and-act feedback mechanism exemplify a closed-loop system, minimizing delays and off-target effects associated with conventional administration. Thus, monitoring and treatment hydrogel MNs embody a transformative approach towards personalized, autonomous, and efficient biomedical interventions.

7.3. Personalized medical

The convergence of medical imaging and advanced manufacturing is paving the way for a new generation of personalized cardiac therapeutics. The fabrication of customized MNs based on patient-specific 3D anatomical data, derive from magnetic resonance imaging [140] (Figure 5D), represent a paradigm shift from one-size-fits-all devices to truly personalized medical solutions [141,142]. This strategy effectively eliminates mechanical mismatch between the device and myocardial tissue by constructing patient-specific cardiac patches, thereby significantly enhancing patch compliance and retention while preventing device displacement. The patch precisely covered the infarct border zone, enabling spatially targeted therapy at critical pathological sites. This approach combines the advantages of individualized configuration with localized drug delivery, allowing sustained high drug concentrations at the target location while reducing systemic exposure, ultimately maximizing therapeutic efficacy. In conclusion, 3D-

printed, anatomy-specific MN patches represented a transformative platform for cardiac regenerative medicine, moving beyond generic designed to offer powerful, personalized approach for treating myocardial infarction and heart failure.

7.4. Functionalization drug delivery strategies

The administration of single medication through either systemic or localized pathways represent a crucial and essential strategy for intervention [143-145]. The foundation of this method revolves around the use of targeted drug molecules designed to accurately engage a specific link in the pathological sequence associated with MI. Han group [146] engineers a multifunctional nanocarrier known as MnO_2@INN@Alb (MIA) that can react to the acidic, hydrogen peroxide-rich environment present at MI sites, facilitating the on-demand production of oxygen and the release of glibenclamide (INN). The MIA inhibits NLRP3-mediated CMs apoptosis while mitigating hypoxia, decreases infarct fibrosis, and enhances myocardial vascular remodeling (Figure 6A). Nevertheless, the effectiveness and constraints of this monotherapy delivery approach arise from its single-target characteristic. Although it demonstrates a clear pharmacological effect, its efficacy is inherently limited by a singular mechanism of action, which is inadequate to address the complex and interconnected pathological cascades that occur post MI. Consequently, monotherapy delivery holds irreplaceable value as a research tool for elucidating pathological mechanisms and validating target feasibility, and plays a critical role in specific clinical scenarios, as well as starkly reveals the inherent challenges in treating complex cardiovascular diseases. This provides a robust theoretical foundation for combination therapies, sequential treatment approaches, or the development of novel drugs with multiple pharmacological actions.

Sequential therapy emerges as an innovative, more targeted therapeutic paradigm [147]. This strategy emphasizes the sequential application of specific interventions tailored to the predominant mechanisms at different stages following MI, thereby maximizing therapeutic efficacy while minimizing adverse effects. He et al. [45] ingeniously design the microencapsulated microneedle patch ($MNP^{Sustain}$) for the sequential delivery of methylprednisolone (Mp), interleukin-10 (IL-10), and VEGF with the goal of improving cardiac function in a rat MI model. In vitro experiment results confirm the sequential release of drugs: Mp is discharged within 3 d, IL-10 is released over a period of 1 to 15 d, while VEGF is gradually released between 3 and 25 d (Figure 6B). Sequential therapy relies on a profound understanding of the precise temporal dynamics of molecular networks across post-MI stages, alongside the capability to assess the progression of pathological processes in vivo in real time. Despite challenges such as determining optimal intervention windows, drug delivery efficiency, and individual heterogeneity, integrating multi-omics data with clinical information to construct personalized temporal treatment pathways undoubtedly represents a key future direction for optimizing long-term outcomes in MI. This approach holds promise for achieving comprehensive improvements, extending from saving lives to enhancing quality of life and long-term cardiac function.

Combination therapy for MI involves the simultaneous or sequential administration of two or more drugs with distinct mechanisms of action [148,149]. Diverging from conventional monotherapy, this strategy employs an integrative manner to simultaneously modulate multiple critical MI-related pathways, resulting in a markedly enhanced therapeutic outcome. For instance, Li and Xu groups [150] develop a non-viral nucleic acid delivery system (CPC) designed to target myocardial endothelial cells for the treatment of MI. This system facilitates the co-delivery of siR-ICAM1, which inhibits inflammation, along with pCXCL12, which encourages

angiogenesis. Furthermore, the CPC is composed of a cationic polymer that has been modified with CRPPR peptides, allowing for precise targeting of myocardial endothelial cells (Figure 6C). The results reveal that the combination of therapies markedly enhances cardiac contractility, reduces inflammatory responses, and facilitates angiogenesis, surpassing the effectiveness of monotherapy with individual nucleic acids. The example conclusively demonstrates that combination therapy, through multi-targeted, multidimensional synergistic intervention, enables more comprehensive and effective control of disease progression, forming the cornerstone of modern pharmacological management for MI.

8. Therapeutic Strategies

Some types hydrogel cardiac patches and MNs depend exclusively on their intrinsic mechanical and conductive properties to provide cardioprotective benefits. Hydrogel patches and MNs have been widely used to deliver cells in combination with a broad spectrum of therapeutic agents (including growth factors, exosomes, genes, drugs, and gas signals) to promote cardiac repair. Given their capacity for sustained release, these platforms are particularly promising for patients with defective endogenous repair, potentially broadening the therapeutic scope and improving efficacy.

8.1. Cellular therapy

Research in both preclinical and clinical settings has demonstrated that cellular therapy mitigated myocardial damage after MI and lower the occurrence of HF. The hydrogel MNs had established 3D microenvironment for the cells, which improved their retention within the infarcted area. Although cellular therapies encountered significant clinical hurdles, their fundamental value was derived from the cell regenerative capacity, which enabled a range of therapeutic actions not possible with conventional drugs. Consequently, the advancement of

hydrogel MNs loaded with cells deserves careful consideration. Tang et al. [131] designed a microneedle patch (MN-CSCs) that incorporated cardiac stromal cells (CSCs) aimed at therapy for cardiac regeneration following an acute MI. The patch consisted of a microneedle array fabricated from the biocompatible polymer PVA, with CSCs encapsulated in fibrin gel and integrated onto the microneedle surface. The function of the microneedles was to act as pathways for the release of regenerative factors produced by CSCs into the damaged heart tissue, while also facilitated the absorption of nutrients. In experimental models of MI using both rats and pigs, the MN-CSC patch reduced myocardial cell death, enhanced vascular myogenesis, decreased scar formation, and improved cardiac performance without causing toxicity, thus presenting a novel approach for heart repair (Figure 7A).

8.2. Growth factors

Given the intrinsic constraints of cellular therapies, several researchers have emphasized the importance of delivering essential reparative factors. Taking into account the degradation characteristics of hydrogel MNs, these microneedles can release regenerative agents like neuregulin-1 [151], mesenchymal stromal cell factor [152], platelet-derived growth factor (PDGF), and VEGF [108]. Liang et al. [153] explore the predictive capability of plasma PDGF for both immediate and prolonged major adverse cardiovascular events after discharge in individuals experiencing non-ST-segment elevation MI. Moreover, Zhang et al. [154] create VEGF-C-mRNA-encapsulated lipid nanoparticles, which are administered through intramyocardial injection to encourage the formation of lymphatic vessels post MI, thereby mitigating inflammatory responses and enhancing cardiac repair. The results manifest that the nanoparticles stimulate the formation of functional lymphatic networks, reduce inflammatory cell infiltration, and suppresse pro-inflammatory as well as fibrotic signaling pathways. Consequently, the significant reduction

in infarct size and the marked improvement in cardiac function are observed (Figure 7B). Some researchers have proposed delivering various factors for synergistic modulation, which offer superior reparative outcomes compared to single factors. Rufaihah et al. [155] investigate the efficacy of polyethylene glycol-fibrinogen (PF) hydrogels in sustaining dual delivery of VEGF and angiopoietin-1 (ANG-1) within ischemic hearts to enhance myocardial repair and function (Figure 7C). Furthermore, the complex pathophysiology of MI demanded the combinatorial therapeutic approach, necessitating the unified system that c simultaneously modulate multiple repair processes. Nonetheless, the practicality of achieving the synergistic effect, where the combined impact exceeds that of individual components in clinical settings, and the potential adverse effects of excessive exogenous regenerative factors remain to be validated. Additionally, susceptibility to deactivation, storage requirements at low temperatures, and high costs posed significant limitations to the clinical application of growth factor therapy.

8.3. Exosomes

Extracellular vesicles know as exosomes range in diameter from 40 to 120 nm and possess a lipid bilayer that encapsulated various growth factors, mRNAs, and microRNAs. The perform effectively under challenging ischemic and hypoxic conditions. Numerous investigations have employed extracellular vesicles as carriers for microRNAs, utilizing hydrogel MNs intended for gene therapy applications [156,157]. Although exosomes demonstrate promising potential for MI, their therapeutic effectiveness is restricted due to a brief plasma half-life. When directly injected into the infarcted region, the exosomes undergo swift metabolic clearance. Hydrogel MNs serve as platforms that enable the localized and sustained storage and release of exosomes. Yuan and colleagues [156] employ exosomes derived from human umbilical cord mesenchymal stem cells (MSCs) as vectors for gene delivery. The research use electroporation to facilitate the

introduction of the microRNA-29b mimic, which is subsequently incorporated onto gelatin-based microneedle patch through the soaking technique (Figure 7D). Following the injected of the MN into the infarcted zone, exosome retention rates are significantly enhanced. Furthermore, the process involved the upregulation of miR-29b expression and the inhibition of fibrosis-associated proteins, which together alleviate inflammation, reduce infarct size, and improve cardiac function. Despite the growing interest in exosomes for MI, their clinical translation is hindered by challenges associated with preparation and large-scale production.

8.4. Gene therapy

Hydrogel MNs serve as platforms for the targeted delivery of therapeutic genes into the infarct zone. Chen et al. [117] construct a nanoparticle-patch system consisting of ZIF-8 nanoparticles and conductive microneedle patches, enabling the localized, efficient, and sustained administration of miR-30d in a rat model of myocardial ischemia-reperfusion injury model (Figure 8A). The ZIF-8 nanoparticles protect miR-30 d from lysosomal degradation within lysosomes through a proton sponge effect [158], while the conductive MN patch facilitate localized drug delivery and release gold nanoparticles to restore electrical conductivity in the damaged myocardium. Recombinant adeno-associated virus (AAV) vectors have garnered significant interest in the gene therapy field due to their advantageous properties. A key advantage of these vectors is their low immunogenicity, which allows them to largely evade detection by the host immune system. This property facilitates prolonged transgene expression, thereby ensuring lasting therapeutic efficacy from a single administration. Additionally, AAV vectors exhibit reduced pathogenicity, made them safer options for delivering genetic material without inducing adverse effects in the host. Within the diverse family of AAV serotypes, include variants such as AAV1, AAV6, and AAV9 have shown remarkable ability to transduce

CMs within the heart tissue. Among these serotypes, AAV9 emerge as the preferred vector for cardiac gene therapy owing to its superior ability to transduce cardiac cells, with high delivery efficiency being pivotal for successful therapeutic outcomes [159]. A PVA-based microneedle patch is uniformly coated with an AAV vector that encode VEGF by Shi et al. [160], result in a significant reduction in infarct area and enhancement of cardiac function in a rat model of MI (Figure 8B). Nonetheless, the application of genetic engineering faces ongoing debates across various fields, particularly within medicine and the food sector, where securing approval from the US Food and Drug Administration is challenging, and ensuring safety validation remains essential.

The investigation of combination therapies that merge our targeted delivery platform with innovative technologies like gene editing and cellular reprogramming signifies a groundbreaking approach to collectively improve myocardial repair. Although the platform is proficient in providing localized and prolonged drug release, its therapeutic capabilities can be significantly enhanced by the simultaneous delivery of advanced molecular agents. For instance, the team led by Wang [161] examines whether the endogenous genes Gata4, Nkx2.5, and Tbx5 can be rapidly activated in adult cardiac fibroblasts in vitro through the CRISPR activation system, thereby establishing autonomous regulatory circuits and initiating the formation of cardiac progenitor cells (CPCs) (Figure 8C). The results manifest that the ciCPCs can differentiate into functional CMs and vascular cells in vitro. In a rat myocardial infarction model, the ciCPCs improve cardiac contractility and reduce scar formation, providing a novel cellular source for cardiac regenerative therapy. Furthermore, Park et al. [162] create a system of CRISPR/Cas9 magnetoplexes (Figure 8D), which is directed to the heart using magnetic field guidance to facilitate in vivo therapeutic genome editing aimed at treating MI. This innovative approach

focuses on the miR34a gene, leading to marked improvements in cardiac repair and regeneration, as well as enhance cardiac function in vivo. Additionally, the method of controlled and localized delivery of CRISPR-Cas9 components allows for accurate *in situ* modification of genes implicated in fibrosis or apoptosis, thus directly mitigate pathological processes in the affected area. At the same time, the platform is perfectly designed for introducing elements that promote cardiac reprogramming, enabling the direct transformation of resident cardiac fibroblasts into functional CMs within the MI environment [163]. Furthermore, this strategy addresses challenges associated with cell transplantation, such as low engraftment rates and the risk of immune rejection. Simultaneously, the approach effectively shields potent yet labile biological agents from systemic degradation, thereby sustaining high local concentrations and prolonging their presence at the target site. Thus, the combined strategy of integrating precise physical targeting with transformative molecular interventions promise to advance beyond mere symptomatic management, paving the way for authentic cardiac regeneration.

There is growing interest in CMs metabolism to re-activate their proliferative capacity. Inspired by regenerative animal models like zebrafish, researchers are exploring strategies to shift adult CMs from oxidative phosphorylation back to glycolysis, a metabolic state that supports cell cycle re-entry [164]. The approach seeks to unlock the endogenous regenerative potential of the heart by modulating its metabolic state. Furthermore, the results reveal that in the context of dilated cardiomyopathy, fibroblasts could worsen the progression of the disease via a maladaptive feedback mechanism. These cells not only deposit surplus extracellular matrix but also contribute to the mechanical stiffness of heart by employing their own cell bodies to support the deteriorating tissue [165]. Targeting specific pathways in these fibroblasts, including p38 signaling, has demonstrated the capacity to alleviate the detrimental process and enhance cardiac

function in models [166], underscoring the importance of fibroblasts as a key therapeutic target in addition to reprogramming. Zhang et al. [167] examine the epigenetic profile of the heart post MI by combining single-cell RNA sequencing with single-cell transposase-accessible chromatin sequencing (scRNA-seq). In rat models of MI, two new subpopulations of fibroblasts are discovered: GATA5/ISL1+ fibroblasts and Gli3high fibroblasts. The GATA5/ISL1+ fibroblasts display characteristics of both fibroblasts and CMs and are crucial for cardiac repair processes. By promoting the trans differentiation of fibroblasts into functional CMs via regulation of the Wnt signaling pathway, the upregulation of GATA5 and ISL1 consequently improve cardiac function and attenuate fibrosis in MI. These findings point to a significant trend in MI research that emphasize multi-targeted and precise therapeutic approaches. The emphasis is on managing the immune microenvironment, reprogramming cell identity directly, improving the delivery of therapeutic agents, and exploring new signaling pathways to foster true cardiac repair and regeneration.

8.5. Gas therapy

Gas therapy represent a novel strategy for treating MI, emphasizing the unique physiological functions of naturally occurring gaseous signaling molecules [168]. Among these are nitric oxide (NO) [169], carbon monoxide (CO) (Figure 9A), oxygen (O_2) (Figures 9B and 9C) [170,171] and hydrogen sulphone (H_2S). The goal of this approach is to tackle myocardial ischemia, mitigate reperfusion injury, and manage the subsequent pathological remodeling processes by utilizing synergistic effects across various pathways. The main function of NO extends beyond safeguarding mitochondria to reducing ROS overproduction, preventing platelet aggregation and leukocyte infiltration, ultimately modulating the ensuing inflammatory cascade [172,173]. The administration of CO contribute to the reduction in MI area by stimulating mitochondrial

biogenesis and suppressing NLRP3 inflammasome activation [174]. Similarly, H_2S influence macrophage phenotypes and regulate signaling pathways that facilitate cardiac fibrosis induced by MI and hypertension (Figures 9D and 9E) [175,176]. However, the clinical application of these gas molecules is limited by their short retention times, poor target specificity, and significant systemic side effects. The hydrogel MNs serve as an effective platform for the safe, localized delivery of prodrug forms of these molecules, enabling controlled release at the target site [138]. For example, Zhu et al. [177] design the nitrate-functionalized cardiac patch to achieve localized NO delivery by covalently attaching nitrate pharmacophore groups to biodegradable polymer. Furthermore, the patch release NO through progressive bioconversion within the ischemic microenvironment implantation into the myocardium, targeting mitochondria to exert cardioprotective effects and promote cardiac repair. Additionally, this team [178] prepare a novel ROS response injectable CS-B-NO hydrogel by releasing NO, thereby regulating the ROS/NO imbalance following I/R injury. More important, the injectable CS-B-NO hydrogel effectively mitigate cardiac injury and improve cardiac function, demonstrate superior efficacy compared to hydrogels releasing NO alone (Figure 9F). Current research focuses on the development of intelligent and responsive gas delivery systems designed to achieve controlled and sustained release of gas molecules at the MI site. This approach maximizes therapeutic efficacy while minimizing potential systemic side effects. Gas therapeutic strategies present novel avenues for regenerative medicine in the context of MI.

8.6. Nano-enzymes therapy

Beyond the aforementioned payloads, enzymes and nanozymes have recently emerged as attractive candidates for MN-mediated delivery in MI [179]. Nanozymes, in particular, offer intrinsic enzyme-mimicking activities (superoxide dismutase (SOD)- and catalase-like (CAT)

functions) that can effectively scavenge ROS and alleviate inflammatory damage in the infarcted heart. For instance, Wang et al. [180] develop the MN patch loaded with a microfluidic-synthesized ZnSBS hybrid gas-nanozyme delivers pH-responsive H_2S and SOD to the infarcted heart, synergistically scavenging ROS, polarizing M2 macrophages, and improving cardiac function after MI (Figure 10A). Additionally, Wang team [181] develop a bilayer microneedle patch (Ce-CLMs-BMN) that responds to both ROS and ultrasound for treating AMI. The upper layer releases CeO_2 nanoparticles to rapidly scavenge ROS and produce oxygen during the acute phase, reducing oxidative stress and inflammation (Figure 10B). The lower layer releases NO upon ultrasound stimulation during the chronic phase, promoting blood vessel growth and preventing heart remodeling. In rat models, this dual-layer, sequential treatment effectively improves cardiac function after AMI. Several recent studies have validated the feasibility of this approach (Figure 10C) [182,183] and some applications have also been found in other fields (Figure 10D) [184,185]. Compared to natural enzymes, nanozymes exhibit higher stability and tunable activity, making them particularly suitable for sustained local delivery via MNs. However, nanozyme hydrogel MNs for MI still have several limitations. First, nanozymes lack the selectivity of natural enzymes and may work efficiently in the complex, acidic, and hypoxic environment of the infarcted heart. Second, the long-term safety of metal-based nanozymes remains unclear, including risks of metal ion leakage, chronic inflammation, and abnormal heart rhythms. Finally, large-scale production, sterilization, and regulatory approval for this combined device-drug product are difficult and expensive.

9. Summary and Outlook

This review focuses on hydrogel MN approaches for MI treatment. It aims to provide researchers with a comprehensive overview of their role in cardiac regeneration and to offer new

perspectives for future studies. Consequently, the hydrogel MN techniques summarized herein hold transformative potential for MI therapy. These hydrogel MNs offer minimally invasive therapeutic solutions that mimic the natural environment of heart to provide mechanical support and therapeutic benefits while mitigating inflammation and fibrosis, and prolonging the efficacy of therapeutic drugs. Beyond the current focus on hydrogel MNs as homogeneous delivery vehicles, an emerging and conceptually distinct approach is the deliberate engineering of heterogeneous MN arrays to match the spatial and functional complexity of diseased tissue. Inspired by a recent study that explored heterogeneous MN arrays for other applications, next-generation cardiac patches could integrate region-specific MNs within a single array: for example, stiffer needles with anti-fibrotic agents for the dense infarct core, and softer, pro-angiogenic or immunomodulatory needles for the border zone. Embracing such structural or functional heterogeneity may unlock new therapeutic paradigms that more faithfully address the multifaceted pathology of MI. As research into these biomaterials deepens, it has become evident that thoroughly understanding the post-infarction mechanisms is paramount. Researchers are now developing novel hydrogel microneedles that not only encapsulate reparative compounds but also function as regenerative scaffolds for damaged myocardial tissue. However, hydrogel MN technology despite remarkable progress in cardiovascular interventional therapy, there are still many challenges to overcome. For example, balance in the mechanical properties of MNs represents a critical challenge, as they must possess sufficient rigidity to penetrate myocardial tissue while maintaining adequate flexibility to match the complex and dynamic physiological environment of the heart. Beyond material and structural innovations, data-driven approaches such as machine learning (ML) are beginning to address the inherent trade-off between mechanical rigidity and flexibility. In addition, the degradability of material and the possible

impacts of its degradation products on the myocardium is a matter of long-term safety concern. The aspect of clinical applicability continues to pose a significant challenge, particularly in ensuring precise implantation through cardiac catheters or minimally invasive surgical techniques. The integration of monitoring capabilities within hydrogel MNs presents an exciting frontier, with the potential to revolutionize healthcare through early intervention and personalized medicine. Although challenges persist, the significant potential for clinical translation underscores its importance as a critical area for future research. From an authoritative perspective, the future of hydrogel MN technology for cardiac repair lies in three paradigm-shifting directions, rather than merely solving material challenges. First, the next generation of hydrogel MNs should evolve from passive therapeutic patches into intelligent closed-loop systems. By integrating flexible sensors (pH, ROS, or cytokines), hydrogel MNs can not only deliver drugs but also monitor the post-infarction microenvironment in real time and trigger on-demand release of reparative factors. This would transform current one-size-fits-all interventions into personalized, feedback-driven therapies. Second, translating hydrogel MNs from bench to bedside requires a rethink of deployment strategies. While current efforts focus on improving mechanical properties (rigidity and flexibility), the real bottleneck is catheter-based, minimally invasive delivery under beating-heart conditions. Therefore, the development of shape-memory or thermos-responsive hydrogel MNs that can be folded into a catheter and self-expand upon contact with the myocardium, eliminating the need for open-chest surgery, is prioritized. Third, the most authoritative vision for long-term safety is merely proving degradability, but achieving beneficial degradation. Instead of inert byproducts, future hydrogel MN degradation should release cardioprotective metabolites (oligopeptides, exosome-mimetic nanoparticles) that actively suppress fibrosis and promote electromechanical coupling of regenerated

cardiomyocytes. This would turn the traditional concern of degradation products into a therapeutic advantage. In summary, hydrogel MN technology will achieve transformative clinical impact by moving beyond incremental optimization of existing designs toward embracing closed-loop intelligence, minimally invasive deploy ability, and beneficial degradation as integrated goals. The outlook presented here provides a clear, authoritative roadmap for researchers and clinicians.

Authorship Contribution Statement

The manuscript was written with the contributions of all authors. All authors have approved the final version of the manuscript.

Xiaofeng Ding, Yongxian Lai and Dequn Wu conceived the idea for this review. Image plotting was conducted by Menghui Chen, Minyue Zhang, Huipeng Wang, Jie Zhu, Hao Liu, Langqun Tan, Xiaoshun Yao, Le kang, and Chenggong Zhang. Jianxiang Li drafted the initial manuscript, while all coauthors provided critical feedback and revisions to the final version. All authors reviewed the manuscript.

Acknowledgments

This work was partially supported by the National Key Research and Development Program of China (project number: 2017YFB0309001) and the Natural Science Foundation of Shanghai (18ZR1400400, 18ZR1400500, 20ZR1402100).

Declaration of Competing Interest

The authors declare that they have no known competing financial interests or personal relationships that could have appeared to influence the work reported in this paper.

Data Availability Statement

No primary research results, software or code have been included and no new data were generated or analyzed as part of this review.

References

[1] Zhao J, Chen Y, Qin Y, et al. Adhesive and conductive hydrogels for the treatment of myocardial infarction. *Macromol. Rapid Commun.* 2025; 46: 2400835.DOI: 10.1002/marc.202400835.

[2] Liu T, Hao Y, Zhang Z, et al. Advanced cardiac patches for the treatment of myocardial infarction. *Circulation*. 2024; 149: 2002-2020.DOI: 10.1161/CIRCULATIONAHA.123.067097.

[3] Roth GA, Mensah GA, Johnson CO, et al. Global burden of cardiovascular diseases and risk factors, 1990–2019: update from the GBD 2019 study. *J. Am. Coll. Cardiol.* 2020; 76: 2982-3021.DOI: 10.1016/j.jacc.2020.11.010.

[4] Cao Y, Fan R, Zhu K, et al. Advances in functionalized hydrogels in the treatment of myocardial infarction and drug-delivery strategies. *ACS Appl. Mater. & Interfaces*. 2024; 16: 48880-48894.DOI: 10.1021/acsami.4c09623.

[5] Yi B, Xu Y, Wang X, et al. Overview of injectable hydrogels for the treatment of myocardial infarction. *Cardiovasc. Innovations*. 2024; 9: 960.DOI: 10.15212/CVIA.2024.0019.

[6] Hua Y, Zeng J, He S, et al. κ-Carrageenan and hyaluronic acid composite injectable hydrogel-containing isosorbide mononitrate-loaded liposomes for treatment of myocardial infarction. *Biomed. Phys. Eng. Express*. 2025; 11: 045008.DOI: 10.1088/2057-1976/adde67.

[7] Zhang J, Guo Y, Bai Y, et al. Application of biomedical materials in the diagnosis and treatment of myocardial infarction. *J. Nanobiotechnol.* 2023; 21: 298.DOI: 10.1186/s12951-023-02063-2.

[8] Ding N, Zheng Z, Zhang CJFiP. Therapeutic potential of human umbilical cord mesenchymal stem cell-derived exosomes in myocardial infarction: from molecular mechanisms to clinical translation-an update. *Front. Pharmacol.* 2025; 16: 1667140.DOI:

10.3389/fphar.2025.1667140.

[9] Janakiram NB, Valerio MS, Goldman SM, et al. The role of the inflammatory response in mediating functional recovery following composite tissue injuries. *Int. J. Mol. Sci*. 2021; 22: 13552.DOI: 10.3390/ijms222413552.

[10] Yang P, Shi Y, Hu H, et al. Inhibition of neuron and cardiac remodeling by microenvironment-responsive injectable hydrogels with sympatho-immune regulation properties for myocardial infarction therapy. *Compos Part B: Eng.* 2025; 297: 112300.DOI: 10.1016/j.compositesb.2025.112300.

[11] Saba L, Libby P. Myocardial infarction, stroke and arterial stenosis: time to reassess a major misunderstanding. *Nat. Rev. Cardiol.* 2025; 1-12.DOI: 10.1038/s41569-025-01186-3.

[12] Mu L, Dong R, Li C, et al. ROS responsive conductive microspheres loaded with salvianolic acid B as adipose derived stem cell carriers for acute myocardial infarction treatment. *Biomaterials*. 2025; 314: 122849.DOI: 10.1016/j.biomaterials.2024.122849.

[13] Wang H, Li L, Luo L, et al. Advanced nanomaterial platforms for targeted therapy of myocardial ischemia–reperfusion injury. *Research*. 2025; 8: 0822.DOI: 10.34133/research.0822.

[14] Lu Y, Yang S, Yang Q, et al. Multifunctional hydrogel strategies for myocardial infarction: from tissue repair to cardiac regeneration. *Adv. Ther.* 2025; 8: 2400383.DOI: 10.1002/adtp.202400383.

[15] Heuts S, Sardari Nia P. Periprocedural myocardial infarction: a web of definitions. *European Journal of Cardio-Thoracic Surgery*. 2021; 60: 443-447.DOI: 10.1093/ejcts/ezab306.

[16] Bei Y, Wang L, Ding R, et al. Animal exercise studies in cardiovascular research: current knowledge and optimal design—A position paper of the Committee on Cardiac Rehabilitation,

Chinese Medical Doctors' Association. *J. Sports Health Sci.* 2021; 10: 660-674.DOI: 10.1016/j.jshs.2021.08.002.

[17] Gabriel-Costa D. The pathophysiology of myocardial infarction-induced heart failure. *Pathophysiology*. 2018; 25: 277-284.DOI: 10.1016/j.pathophys.2018.04.003.

[18] Pagliaro BR, Cannata F, Stefanini GG, et al. Myocardial ischemia and coronary disease in heart failure. *Heart Failure Rev.* 2020; 25: 53-65.DOI: 10.1007/s10741-019-09831-z.

[19] Luo X, Zhong Z, Chong A, et al. Function and mechanism of trimetazidine in myocardial infarction-induced myocardial energy metabolism disorder through the SIRT1-AMPK pathway. *Front. Physiol.* 2021; 12: 645041.DOI: 10.3389/fphys.2021.645041.

[20] She P, Gao B, Li D, et al. The transcriptional repressor HEY2 regulates mitochondrial oxidative respiration to maintain cardiac homeostasis. *Nat. Commun.* 2025; 16: 232.DOI: 10.1038/s41467-024-55557-4.

[21] Gibb AA, Hill BG. Metabolic coordination of physiological and pathological cardiac remodeling. *Circ. Res.* 2018; 123: 107-128.DOI: 10.1161/CIRCRESAHA.118.312017.

[22] Wang F, Xu Z, Zheng F, et al. Cardiac organoid model inspired micro-robot smart patch to treat myocardial infarction. *Adv. Mater.* 2025; 37: 2417327.DOI: 10.1002/adma.202417327.

[23] Morris G, Walker A, Berk M, et al. Cell death pathways: a novel therapeutic approach for neuroscientists. *Mol. Neurobiol.* 2018; 55: 5767-5786.DOI: 10.1007/s12035-017-0793-y.

[24] Damluji AA, Van Diepen S, Katz JN, et al. Mechanical complications of acute myocardial infarction: a scientific statement from the American heart association. *Circulation*. 2021; 144: e16-e35.DOI: 10.1161/CIR.0000000000000985.

[25] Peet C, Ivetic A, Bromage DI, et al. Cardiac monocytes and macrophages after myocardial infarction. *Cardiovasc. Res.* 2020; 116: 1101-1112.DOI: 10.1093/cvr/cvz336.

[26] Contessotto P, Pandit A. Therapies to prevent post-infarction remodelling: From repair to regeneration. *Biomaterials*. 2021; 275: 120906.DOI: 10.1016/j.biomaterials.2021.120906.

[27] Ling C, Chen L, Liang J, et al. Neutrophil/monocyte-targeted dual-ligands modified liposomes delivering puerarin for ischemia stroke treatment. *Mater. Today Bio*. 2025; 33: 102077.DOI: 10.1016/j.mtbio.2025.102077.

[28] Zabihi A. The role of biological macromolecules in the regulation of angiogenesis in glioblastoma: Focus on vascular growth factors, integrins, and extracellular matrix proteins. *Int. J. Biol. Macromol.* 2025; 311: 143838.DOI: 10.1016/j.ijbiomac.2025.143838.

[29] Frangogiannis NG. The inflammatory response in myocardial injury, repair, and remodelling. *Nat. Rev. Cardiol.* 2014; 11: 255-265.DOI: 10.1038/nrcardio.2014.28.

[30] Zhang Q, Wang L, Wang S, et al. Signaling pathways and targeted therapy for myocardial infarction. *Signal Transduction Targeted Ther.* 2022; 7: 78.DOI: 10.1038/s41392-022-00925-z.

[31] Dubey N, Vishwakarma VK, Verma A, et al. Cardiac fibroblast receptors: a preclinical dive into their regulatory influence on cardiovascular diseases. *J. Biochem. Mol. Toxicol.* 2025; 39: e70347.DOI: 10.1002/jbt.70347.

[32] Wu T, Liu W. Functional hydrogels for the treatment of myocardial infarction. *NPG Asia Mater.* 2022; 14: 9.DOI: 10.1038/s41427-021-00330-y.

[33] Zhang X, Zhang Y, Liu Y. Fibroblast activation and heterogeneity in fibrotic disease. *Nat. Rev. Nephrol.* 2025; 21: 1-20.DOI: 10.1038/s41581-025-00969-8.

[34] Wang X, Yu S, Xie L, et al. The role of the extracellular matrix in cardiac regeneration. *Heliyon*. 2025; 11: e41157.DOI: 10.1016/j.heliyon.2024.e41157.

[35] Weber KT, Sun Y, Bhattacharya SK, et al. Myofibroblast-mediated mechanisms of

pathological remodelling of the heart. *Nat. Rev. Cardiol.* 2013; 10: 15-26.DOI: 10.1038/nrcardio.2012.158.

[36] Gourdie RG, Dimmeler S, Kohl P. Novel therapeutic strategies targeting fibroblasts and fibrosis in heart disease. *Nat. Rev. Drug Discovery*. 2016; 15: 620-638.DOI: 10.1038/nrd.2016.89.

[37] Shilo M, Oved H, Wertheim L, et al. Injectable nanocomposite implants reduce ROS accumulation and improve heart function after infarction. *Adv. Sci.* . 2021; 8: 2102919.DOI: 10.1002/advs.202102919.

[38] Aksentijevic D, Sedej S, Fauconnier J, et al. Mechano-energetic uncoupling in heart failure. *Nat. Rev. Cardiol.* 2025; 22: 1-25.DOI: 10.1038/s41569-025-01167-6.

[39] Fu L, Han K, Qi J, et al. Electrohydrodynamically-printed serpentine fiber scaffolds with enhanced conductivity and elasticity for post-myocardial infarction repair. *Acta Biomater.* 2025; 200: 476-488.DOI: 10.1016/j.actbio.2025.05.014.

[40] Lin M, Qin J, Lin S, et al. Bioengineered hydrogels for restoring cardiac electronic activity after myocardial infarction. *Adv. Healthcare Mater.* 2025; 14: 2502058.DOI: 10.1002/adhm.202502058.

[41] Yang Y, Lei D, Huang S, et al. Elastic 3D-printed hybrid polymeric scaffold improves cardiac remodeling after myocardial infarction. *Adv. Healthcare Mater.* 2019; 8: 1900065.DOI: 10.1002/adhm.201900065.

[42] Huang S, Lei D, Yang Q, et al. A perfusable, multifunctional epicardial device improves cardiac function and tissue repair. *Nat. Med.* . 2021; 27: 480-490.DOI: 10.1038/s41591-021-01279-9.

[43] Bai L, Luo Q, Gao Z, et al. Bioinspired conductive structural color hydrogels: a theragnostic

platform for spatiotemporal monitoring and repair of myocardial infarction. *Adv. Funct. Mater.* 2025; 35: 10548.DOI: 10.1002/adfm.202510548.

[44] Melvinsdottir IH, Midgett D, Lee SR, et al. Intramyocardial hydrogel delivery decreases left ventricular remodeling and increases angiogenesis post myocardial infarction. *Circulation: Cardiovasc. Imagin*. 2025; 18: e018357.DOI: 10.1161/CIRCIMAGING.125.018357.

[45] He F, Andrabi SM, Shi H, et al. Sequential delivery of cardioactive drugs via microcapped microneedle patches for improved heart function in post myocardial infarction rats. *Acta Biomater.* 2025; 192: 235-247.DOI: 10.1016/j.actbio.2024.12.009.

[46] Liu Q, Zhao R, Zhang D, et al. Biodegradable microneedle patch confers crocin with outstanding effects in the treatment of myocardial infarction. *ACS Omega*. 2025; 10: 14176-14187.DOI: 10.1021/acsomega.4c11540.

[47] Fei Y, Liu X, Zhai M, et al. A two-stage nanoengineered microneedle platform for on-demand tumor-microenvironment-responsive therapy and enhanced wound healing against postoperative breast cancer recurrence. *Med Mat*. 2026; 3: 96-113.DOI: 10.1097/mm9.0000000000000035.

[48] Li S, Yin W, Liu Y, et al. Anisotropic conductive scaffolds for post-infarction cardiac repair. *Biomater. Sci.* 2025; 13: 542-567.DOI: 10.1039/D4BM01109K

[49] Wang L, Liu Y, Ye G, et al. Injectable and conductive cardiac patches repair infarcted myocardium in rats and minipigs. *Nat. Biomed. Eng.* 2021; 5: 1157-1173.DOI: 10.1038/s41551-021-00796-9.

[50] Chen J, Zhan Y, Wang Y, et al. Chitosan/silk fibroin modified nanofibrous patches with mesenchymal stem cells prevent heart remodeling post-myocardial infarction in rats. *Acta Biomater.* 2018; 80: 154-168.DOI: 10.1016/j.actbio.2018.09.013.

[51] Yao Y, Li A, Wang S, et al. Multifunctional elastomer cardiac patches for preventing left ventricle remodeling after myocardial infarction in vivo. *Biomaterials*. 2022; 282: 121382.DOI: 10.1016/j.biomaterials.2022.121382.

[52] Kim J, Cha GD, Kim M, et al. Soft cardiac patch using a bifacial architecture of adhesive/low-impedance hydrogel nanocomposites and highly conductive elastomer nanocomposites. *Adv. NanoBiomed Res.* 2025; 5: 2400143.DOI: 10.1002/anbr.202400143.

[53] Wang Y, Chen G, Zhang H, et al. Emerging functional biomaterials as medical patches. *ACS Nano*. 2021; 15: 5977-6007.DOI: 10.1021/acsnano.0c10724.

[54] Dong S, An S, Saiding Q, et al. Therapeutic hydrogels: properties and biomedical applications. *Chem. Rev.* 2025; 125: 8835-8920.DOI: 10.1021/acs.chemrev.5c00182.

[55] Mao Y, Sun P, Yin X, et al. Conductive microneedle patch with mitochondria-localized generation of nitric oxide promotes heart repair after ischemia-reperfusion therapy. *Small Methods*. 2025; 9: e00818.DOI: 10.1002/smtd.202500818.

[56] Yevtushenko P, Kuehne T, Bruening J, et al. A simulation-based comparison of human, porcine and ovine pulmonary artery hemodynamics. Evaluating the suitability of large animal models for endopulmonary device evaluation from a hemodynamics point of view. *Cardiovasc. Eng. Technol.* 2025; 16: 688-702.DOI: 10.1007/s13239-025-00803-z.

[57] Jin Q, Wang Y, Lei W, et al. A core-shell structured biphasic microneedle system as an elite squad for combating melanoma with “three-in-one” therapeutic power. *Biomater. Sci.* 2025; 13: 3662-3677.DOI: 10.1039/D5BM00371G

[58] Shah SWA, Li X, Yuan H, et al. Innovative transdermal drug delivery systems: benefits, challenges, and emerging application. *BMEMat*. 2025; e70001.DOI: 10.1002/bmm2.70001.

[59] Ghosh A, Sanyal A, Kumari M, et al. Innovations in additive manufacturing approaches for

the fabrication of advanced drug delivery platforms, biomimetics, and predictive 3D microphysiological interfaces. *J. Mater. Chem. B*. 2025; 13: 11928-11970.DOI: 10.1039/D5TB01170A.

[60] Liu L, Wang F, Chen X, et al. Designing multifunctional microneedles in biomedical engineering: materials, methods, and applications. *Int. J. Nanomed.* 2025; 20: 8693-8728.DOI: 10.2147/IJN.S531898.

[61] Gerstel M, Place V, inventors; Drug delivery device. Google Patents. 1976.

[62] Waghule T, Singhvi G, Dubey SK, et al. Microneedles: A smart approach and increasing potential for transdermal drug delivery system. *Biomed. Pharmacother.* 2019; 109: 1249-1258.DOI: 10.1016/j.biopha.2018.10.078.

[63] Rzhevskiy AS, Singh TRR, Donnelly RF, et al. Microneedles as the technique of drug delivery enhancement in diverse organs and tissues. *J. Controlled Release*. 2018; 270: 184-202.DOI: 10.1016/j.jconrel.2017.11.048.

[64] Donnelly RF, Singh TRR, Garland MJ, et al. Hydrogel-forming microneedle arrays for enhanced transdermal drug delivery. *Adv. Funct. Mater.* 2012; 22: 4879-4890.DOI: 10.1002/adfm.201200864.

[65] Miao M, Wu Q, Zhou X, et al. Interfacing hydrogel microneedle patch for diagnosis. *Surf. Interfaces*. 2024; 55: 105474.DOI: 10.1016/j.surfin.2024.105474.

[66] AlBadry AS, AlMayahy MH, Scurr DJ. Enhanced transdermal delivery of acyclovir via hydrogel microneedle arrays. *J. Pharm. Sci.* 2023; 112: 1011-1019.DOI: 10.1016/j.xphs.2022.11.012.

[67] Gill HS, Denson DD, Burris BA, et al. Effect of microneedle design on pain in human volunteers. *Clin. J. Pain*. 2008; 24: 585-594.DOI: 10.1097/AJP.0b013e31816778f9.

[68] Gittard SD, Chen B, Xu H, et al. The effects of geometry on skin penetration and failure of polymer microneedles. *J. Adhes. Sci. Technol.* 2013; 27: 227-243.DOI: 10.1080/01694243.2012.705101.

[69] Moga KA, Bickford LR, Geil RD, et al. Rapidly-dissolvable microneedle patches via a highly scalable and reproducible soft lithography approach. *Adv. Mater.* 2013; 25: 5060-5066.DOI: 10.1002/adma.201300526.

[70] Römgens A, Bader D, Bouwstra J, et al. Monitoring the penetration process of single microneedles with varying tip diameters. *J. Mech. Behav. Biomed. Mater.* 2014; 40: 397-405.DOI: 10.1016/j.jmbbm.2014.09.015.

[71] Yang J, Liu X, Fu Y, et al. Recent advances of microneedles for biomedical applications: drug delivery and beyond. *Acta Pharm. Sin. B*. 2019; 9: 469-483.DOI: 10.1016/j.apsb.2019.03.007.

[72] Ramöller IK, McAlister E, Bogan A, et al. Novel design approaches in the fabrication of polymeric microarray patches via micromoulding. *Micromachines*. 2020; 11: 554.DOI: 10.3390/mi11060554.

[73] Migdadi EM, Courtenay AJ, Tekko IA, et al. Hydrogel-forming microneedles enhance transdermal delivery of metformin hydrochloride. *J. Controlled Release*. 2018; 285: 142-151.DOI: 10.1016/j.jconrel.2018.07.009.

[74] Caffarel-Salvador E, Brady AJ, Eltayib E, et al. Hydrogel-forming microneedle arrays allow detection of drugs and glucose in vivo: potential for use in diagnosis and therapeutic drug monitoring. *PloS One*. 2015; 10: e0145644.DOI: 10.1371/journal.pone.0145644.g002.

[75] Donnelly RF, Mooney K, Caffarel-Salvador E, et al. Microneedle-mediated minimally invasive patient monitoring. *Ther. Drug Monit.* 2014; 36: 10-17.DOI: 10.1097/FTD.0000000000000022.

[76] Wang M, Hu L, Xu C. Recent advances in the design of polymeric microneedles for transdermal drug delivery and biosensing. *Lab Chip*. 2017; 17: 1373-1387.DOI: 10.1039/C7LC00016B.

[77] Qin J, Hu C, Ran X, et al. Bionic microneedle patch inspired by drosophila tarsal paws boosts healing in bacterial infectious stomatitis. *Adv. Sci.* . 2025; e00432.DOI: 10.1002/advs.202500432.

[78] Zhao J, Lv J, Ling G, et al. A swellable hydrogel microneedle based on cerium-metal organic frame composite nanozyme for detection of biomarkers. *Int. J. Biol. Macromol.* 2024; 254: 127745.DOI: 10.1016/j.ijbiomac.2023.127745.

[79] Wang X, Han C, Xia J, et al. Ultrasound-mediated piezoelectric microneedles regulating macrophage polarization and remodeling pathological microenvironment for lymphedema improvement. *ACS Nano*. 2024; 19: 1447-1462.DOI: 10.1021/acsnano.4c14292.

[80] Kolluru C, Gupta R, Jiang Q, et al. Plasmonic paper microneedle patch for on-patch detection of molecules in dermal interstitial fluid. *ACS Sensors*. 2019; 4: 1569-1576.DOI: 10.1021/acssensors.9b00258.

[81] Shen J, Fu W, Wei W, et al. GO-aptamer hydrogel microneedle sensors for the on-site detection of exosomes in interstitial fluid on acupuncture treatment. *Biosens. Bioelectron.* 2025; 280: 117426.DOI: 10.1021/acs.jmedchem.5c01169.

[82] Singh P, Carrier A, Chen Y, et al. Polymeric microneedles for controlled transdermal drug delivery. *J. Controlled Release*. 2019; 315: 97-113.DOI: 10.1016/j.jconrel.2019.10.022.

[83] Krieger KJ, Bertollo N, Dangol M, et al. Simple and customizable method for fabrication of high-aspect ratio microneedle molds using low-cost 3D printing. *Microsyst. Nanoeng.* 2019; 5: 42.DOI: 10.1038/s41378-019-0088-8.

[84] Kuo S, Chou Y. A novel polymer microneedle arrays and PDMS micromolding technique. *J. Appl. Sci. Eng.* 2004; 7: 95-98.DOI: 10.6180/jase.2004.7.2.08.

[85] Zeng Q, Yang Y, Wang H, et al. 3D printing of structural bionic and functionalized hydrogels for the construction of macroscale human cardiac tissues. *Biomaterials*. 2025; 325: 123573.DOI: 10.1016/j.biomaterials.2025.123573.

[86] Turner JG, White LR, Estrela P, et al. Hydrogel-forming microneedles: current advancements and future trends. *Macromol. Biosci.* 2021; 21: 2000307.DOI: 10.1002/mabi.202000307.

[87] He Y, Li Q, Chen P, et al. A smart adhesive Janus hydrogel for non-invasive cardiac repair and tissue adhesion prevention. *Nat. Commun.* 2022; 13: 7666.DOI: 10.1038/s41467-022-35437-5.

[88] Li J, Yao Y, Zhou J, et al. Epicardial transplantation of antioxidant polyurethane scaffold based human amniotic epithelial stem cell patch for myocardial infarction treatment. *Nat. Commun.* 2024; 15: 9105.DOI: 10.1038/s41467-024-53531-8.

[89] Wei X, Wang L, Duan C, et al. Cardiac patches made of brown adipose-derived stem cell sheets and conductive electrospun nanofibers restore infarcted heart for ischemic myocardial infarction. *Bioact. Mater.* 2023; 27: 271-287.DOI: 10.1016/j.bioactmat.2023.03.023.

[90] Y. Kong LW, F. Duan, et al. Injectable and pH-activated self-feedback hydrogel encapsulating stem cells for augmented acute myocardial infarction therap. *Adv. Healthcare Mater.* 2025; e03324.DOI: 10.1002/adhm.202503324.

[91] Chen W, Wang C, Liu W, et al. A matrix-metalloproteinase-responsive hydrogel system for modulating the immune microenvironment in myocardial infarction. *Adv. Mater.* 2023; 35: 2209041.DOI: 10.1002/adma.202209041.

[92] Wang S, Wang K, Cao W, et al. Treg-enhancing and immunomodulating microgel scaffold

promotes cell ingrowth and heart function recovery post-acute myocardial infarction in vivo. *Chem. Eng. J.* 2024; 497: 154933.DOI: 10.1016/j.cej.2024.154933.

[93] He S, Long L, Wang Z, et al. Combining HUMSC secretome and a conductive hydrogel enhances angiogenesis and electrical transmission at myocardial infarct sites to support cardiac repair. *Chem. Eng. J.* 2023; 474: 145877.DOI: 10.1016/j.cej.2023.145877.

[94] Deng K, Hua Y, Gao Y, et al. Thermosensitive hydrogel with programmable, self-regulated HIF-1α stabilizer release for myocardial infarction treatment. *Adv. Sci.* . 2024; 11: 2408013.DOI: 10.1002/advs.202408013.

[95] Lee K, Xue Y, Lee J, et al. A patch of detachable hybrid microneedle depot for localized delivery of mesenchymal stem cells in regeneration therapy. *Adv. Funct. Mater.* 2020; 30: 2000086.DOI: 10.1002/adfm.202000086.

[96] Fan Z, Wei Y, Yin Z, et al. Near-infrared light-triggered unfolding microneedle patch for minimally invasive treatment of myocardial ischemia. *ACS Appl. Mater. & Interfaces*. 2021; 13: 40278-40289.DOI: 10.1021/acsami.1c09658.

[97] Wang M, Dai T, Zhu D. Design and development of nanoselenium-ruthenium/collagen-loaded multifunctional injectable hydrogel delivery for promising treatment of myocardial infarction. *J. Drug Delivery Sci. Technol.* 2025; 104: 106522.DOI: 10.1016/j.jddst.2024.106522.

[98] Zhao Z, Xu H, Li A, et al. Enalaprilat-loaded polyphenol nanoparticle composite hydrogel promotes myocardial protection after acute infarction. *Compos. Part B: Eng.* 2024; 278: 111430.DOI: 10.1016/j.compositesb.2024.111430.

[99] Wang X, Wang L, Wu Q, et al. Chitosan/calcium silicate cardiac patch stimulates cardiomyocyte activity and myocardial performance after infarction by synergistic effect of bioactive ions and aligned nanostructure. *ACS Appl. Mater. & Interfaces*. 2018; 11: 1449-

1468.DOI: 10.1021/acsami.8b17754.

[100] Wang T, Wang Y, Zhang Y, et al. Drug-loaded mesoporous polydopamine nanoparticles in chitosan hydrogels enable myocardial infarction repair through ROS scavenging and inhibition of apoptosis. *ACS Appl. Mater. & Interfaces*. 2024; 16: 61551-61564.DOI: 10.1021/acsami.4c08155.

[101] Jia X, Liu W, Ai Y, et al. A multifunctional anisotropic patch manufactured by microfluidic manipulation for the repair of infarcted myocardium. *Adv. Mater.* 2024; 36: 2404071.DOI: 10.1002/adma.202404071.

[102] Zhang L, Shao L, Li J, et al. Annexin A1-loaded alginate hydrogel promotes cardiac repair via modulation of macrophage phenotypes after myocardial infarction. *ACS Biomater. Sci. & Eng.* 2024; 10: 3232-3241.DOI: 10.1021/acsbiomaterials.4c00146.

[103] Wang X, Wang J, Zhang Y, et al. A fibrin patch loaded with mesenchymal stem cells-derived exosomes improves cardiac functions after myocardial infarction. *Colloid Interface Sci. Commun.* 2024; 59: 100775.DOI: 10.1016/j.colcom.2024.100775.

[104] Chang T, Liu C, Yang H, et al. Fibrin-based cardiac patch containing neuregulin-1 for heart repair after myocardial infarction. *Colloids Surf., B*. 2022; 220: 112936.DOI: 10.1016/j.colsurfb.2022.112936.

[105] Zhao C, Liu J, Tian Y, et al. A functional cardiac patch with “gas and ion” dual-effect intervention for reconstructing blood microcirculation in myocardial infarction repair. *Biomaterials*. 2025; 321: 123300.DOI: 10.1016/j.biomaterials.2025.123300.

[106] Luo Q, Gao Z, Bai L, et al. Bioactive peptide-based composite hydrogel for myocardial infarction treatment: ROS scavenging and angiogenesis regulation. *Acta Biomater.* 2025; 197: 167-183.DOI: /10.1016/j.actbio.2025.03.035.

[107] Chen H, Fan L, Peng N, et al. Galunisertib-loaded gelatin methacryloyl hydrogel microneedle patch for cardiac repair after myocardial infarction. *ACS Appl. Mater. & Interfaces*. 2022; 14: 40491-40500.DOI: 10.1021/acsami.2c05352.

[108] Lim S, Park TY, Jeon EY, et al. Double-layered adhesive microneedle bandage based on biofunctionalized mussel protein for cardiac tissue regeneration. *Biomaterials*. 2021; 278: 121171.DOI: 10.1016/j.biomaterials.2021.121171.

[109] Wang Y, Wang J, Liu C, et al. Injectable decellularized extracellular matrix hydrogel loaded with exosomes encapsulating curcumin for prevention of cardiac fibrosis after myocardial infarction. *J. Mater. Sci. & Technol.* 2023; 167: 50-58.DOI: 10.1016/j.jmst.2023.06.005.

[110] Kai D, Prabhakaran MP, Jin G, et al. Biocompatibility evaluation of electrically conductive nanofibrous scaffolds for cardiac tissue engineering. *J. Mater. Chem. B*. 2013; 1: 2305-2314.DOI: 10.1039/C3TB00151B.

[111] Yu C, Shi M, He S, et al. Chronological adhesive cardiac patch for synchronous mechanophysiological monitoring and electrocoupling therapy. *Nat. Commun.* 2023; 14: 6226.DOI: 10.1038/s41467-023-42008-9.

[112] Wu C, Zhang Y, Xu Y, et al. Injectable polyaniline nanorods/alginate hydrogel with AAV9-mediated VEGF overexpression for myocardial infarction treatment. *Biomaterials*. 2023; 296: 122088.DOI: 10.1016/j.biomaterials.2023.122088.

[113] He S, Long L, Liu W, et al. A redox-active and electroactive hydrogel enabled by an integrated PEDOT@PMOF nanofiller for post-infarct myocardial repair. *Adv. Sci.* . 2025; 12: e05612.DOI: 10.1002/advs.202505612.

[114] Zhang F, Zhang Y, Qian S, et al. Injectable and conductive nanomicelle hydrogel with α-tocopherol encapsulation for enhanced myocardial infarction repair. *ACS Nano*. 2024; 18:

10216-10229.DOI: 10.1021/acsnano.4c00509.

[115] Sun L, Zhu X, Zhang X, et al. Induced cardiomyocytes-integrated conductive microneedle patch for treating myocardial infarction. *Chem. Eng. J.* 2021; 414: 128723.DOI: 10.1016/j.cej.2021.128723.

[116] Cheng N, Luo Q, Yang Y, et al. Injectable pH responsive conductive hydrogel for intelligent delivery of metformin and exosomes to enhance cardiac repair after myocardial ischemia-reperfusion injury. *Adv. Sci.* . 2025; 12: 2410590.DOI: 10.1002/advs.202410590.

[117] Chen X, Chen H, Zhu L, et al. Nanoparticle-patch system for localized, effective, and sustained MiRNA administration into infarcted myocardium to alleviate myocardial ischemia-reperfusion injury. *ACS Nano*. 2024; 18: 19470-19488.DOI: 10.1021/acsnano.3c08811.

[118] Zhang Y, Xu Y, Wu C, et al. Injectable conductive hydrogel patch with spatiotemporallytailored asymmetric adhesion for myocardial infarction repair. *Adv. Mater.* 2025; e10824.DOI: 10.1002/adma.202510824.

[119] Wang X, Wang H, Liu X, et al. Self-adhesion conductive cardiac patch based on methoxytriethylene glycol-functionalized graphene effectively improves cardiac function after myocardial infarction. *J. Adv. Res.* 2024; 76: 745-759.DOI: 10.1016/j.jare.2024.11.026.

[120] Zhang L, Li T, Yu Y, et al. An injectable conductive hydrogel restores electrical transmission at myocardial infarct site to preserve cardiac function and enhance repair. *Bioact. Mater.* 2022; 20: 339.DOI: 10.1016/j.bioactmat.2022.06.001.

[121] Naguib M, Kurtoglu M, Presser V, et al. Two-dimensional nanocrystals produced by exfoliation of Ti_3AlC_2. MXenes15-29.

[122] Lee M, Park J, Choe G, et al. A conductive and adhesive hydrogel composed of MXene nanoflakes as a paintable cardiac patch for infarcted heart repair. *ACS Nano*. 2023; 17: 12290-

12304.DOI: 10.1021/acsnano.3c00933.

[123] Ren X, Xiao M, Xu Y, et al. Injectable MXene conductive hydrogel improves myocardial infarction through scavenging ROS and repairing myocardium electrical integrity. *Chem. Eng. J.* 2024; 481: 148791.DOI: 10.1016/j.cej.2024.148791.

[124] Engler AJ, Carag-Krieger C, Johnson CP, et al. Embryonic cardiomyocytes beat best on a matrix with heart-like elasticity: scar-like rigidity inhibits beating. *J. Cell Sci.* 2008; 121: 3794-3802.DOI: 10.1242/jcs.029678.

[125] Kitsara M, Agbulut O, Kontziampasis D, et al. Fibers for hearts: A critical review on electrospinning for cardiac tissue engineering. *Acta Biomater.* 2017; 48: 20-40.DOI: 10.1016/j.actbio.2016.11.014.

[126] Serpooshan V, Zhao M, Metzler SA, et al. The effect of bioengineered acellular collagen patch on cardiac remodeling and ventricular function post myocardial infarction. *Biomaterials*. 2013; 34: 9048-9055.DOI: 10.1016/j.biomaterials.2013.08.017.

[127] Chaturvedi RR, Herron T, Simmons R, et al. Passive stiffness of myocardium from congenital heart disease and implications for diastole. *Circulation*. 2010; 121: 979-988.DOI: 10.1161/CIRCULATIONAHA.109.850677.

[128] Mann DL, Kubo SH, Sabbah HN, et al. Beneficial effects of the CorCap cardiac support device: five-year results from the Acorn Trial. *J. Thorac. Cardiovasc. Surg.* 2012; 143: 1036-1042.DOI: 10.1016/j.jtcvs.2011.06.014.

[129] Atluri P, Acker MA. Diastolic ventricular support with cardiac support devices: an alternative approach to prevent adverse ventricular remodeling. *Heart Failure Rev.* 2013; 18: 55-63.DOI: 10.1007/s10741-012-9312-4.

[130] Wu P, Sai X, Li Z, et al. Maturation of induced pluripotent stem cell-derived cardiomyocytes

and its therapeutic effect on myocardial infarction in mouse. *Bioact. Mater.* 2023; 20: 286-305.DOI: 10.1016/j.bioactmat.2022.05.024.

[131] Tang J, Wang J, Huang K, et al. Cardiac cell-integrated microneedle patch for treating myocardial infarction. *Sci. Adv.* . 2018; 4: eaat9365.DOI: 10.1126/sciadv.aat9365.

[132] Cross HR, Clarke K, Opie LH, et al. Is lactate-induced myocardial ischaemic injury mediated by decreased pH or increased intracellular lactate? *J. Mol. Cell. Cardiol.* 1995; 27: 1369-1381.DOI: 10.1006/jmcc.1995.0130.

[133] Lodrini AM, Goumans M-J. Cardiomyocytes cellular phenotypes after myocardial infarction. *Front. Cardiovasc. Med.* 2021; 8: 750510.DOI: 10.3389/fcvm.2021.750510.

[134] Wang VY, Zhu Y, Spaulding KA, et al. NIPAAm-co-PEG4000 thermoresponsive hydrogel with ROS scavenging properties improves in vivo border zone contractility and reduces myocardial remodeling in sheep after MI. *Acta Biomater.* 2025; DOI: 10.1016/j.actbio.2025.06.046.

[135] Zhen P, Jiang Q, Yu F, et al. ROS-differentiated release of Apelin-13 from hydrogel comprehensively treats myocardial ischemia-reperfusion injury. *J. Controlled Release*. 2025; 379: 609-620.DOI: 10.1016/j.jconrel.2025.01.039.

[136] Wang L, Yu C, You T, et al. Injection of ROS-responsive hydrogel loaded with IL-1β-targeted nanobody for ameliorating myocardial infarction. *Bioact. Mater.* 2025; 46: 273-284.DOI: 10.1016/j.bioactmat.2024.12.013.

[137] Zou Z, Gong X, He Z, et al. Wireless ECG monitoring in conscious mice: a valuable tool for investigating cardiac function in myocardial Infarction research. *IEEE Sensors J.* 2024; 24: 41090-41098.DOI: 10.1109/JSEN.2024.3477419.

[138] Yang K, Dong Q, Yao Z, et al. A wearable dual-modal patch for rapid pre-Hospital diagnosis

of acute myocardial infarction. *ACS Nano*. 2025; 19: 23969-23981.DOI: 10.1021/acsnano.5c05461.

[139] Zhang K, Wang P, Wu L, et al. A soft patch for dynamic myocardial infarction monitoring. *ACS Appl. Mater. & Interfaces*. 2025; 17: 16479-16488.DOI: 10.1021/acsami.4c18868.

[140] Li Y, Tuerhan M, Li B, et al. RGD-modified ZIF-8 nanoparticles as a drug carrier for MR imaging and targeted drug delivery in myocardial infarction. *Nanomedicine*. 2024; 19: 1585-1600.DOI: 10.1080/17435889.2024.2365623.

[141] Guo X, Yang D, Wang D, et al. Self-adaptive vision-language model for 3D segmentation of pulmonary artery and vein. Springer; 2025:489-499.

[142] Dhand AP, Davidson MD, Zlotnick HM, et al. Additive manufacturing of highly entangled polymer networks. *Science*. 2024; 385: 566-572.DOI: 10.1126/science.adn6925.

[143] Qiao J, Xu X, Zhou X, et al. Targeted ganglion delivery of CaV2. 2-mediated peptide by DNA nanoflowers for relieving myocardial infarction and neuropathic pain. *ACS Nano*. 2025; 19: 13037-13052.DOI: 10.1021/acsnano.4c17325.

[144] Ma Z, Li M, Guo R, et al. Treating myocardial infarction via a nano-ultrasonic contrast agent-mediated high-efficiency drug delivery system targeting macrophages. *Sci. Adv.* 2025; 11: eadp7126.DOI: 10.1126/sciadv.adp7126.

[145] Wang K, Sun Y, Zhu K, et al. Anti-pyroptosis biomimetic nanoplatform loading puerarin for myocardial infarction repair: from drug discovery to drug delivery. *Biomaterials*. 2025; 314: 122890.DOI: 10.1016/j.biomaterials.2024.122890.

[146] Zhu W, Lu Y, Zong B, et al. Ameliorating myocardial infarction by concurrent pyroptosis suppression and on-demand oxygen production via functionalized nanocarrier. *ACS Appl. Mater. & Interfaces*. 2025; 17: 41626-41636.DOI: 10.1021/acsami.5c01964.

[147] Juengel E, Kim D, Makarević J, et al. Molecular analysis of sunitinib resistant renal cell carcinoma cells after sequential treatment with RAD 001 (everolimus) or sorafenib. *J. Cell. Mol. Med.* 2015; 19: 430-441.DOI: 10.1111/jcmm.12471.

[148] Gao H, Liu S, Qin S, et al. Injectable hydrogel-based combination therapy for myocardial infarction: a systematic review and Meta-analysis of preclinical trials. *BMC Cardiovasc. Disord.* 2024; 24: 119.DOI: 10.1186/s12872-024-03742-0.

[149] Zhou H, Yang Z, Jin G, et al. Polymeric nanoparticles simultaneously delivering paclitaxel prodrug and combretastatin A4 with exceptionally high drug loading for cancer combination therapy. *Nano Lett.* 2025; 25: 3479-3488.DOI: 10.1021/acs.nanolett.4c05863.

[150] Shao Y, Xu C, Zhu S, et al. One endothelium-targeted combined nucleic acid delivery system for myocardial infarction therapy. *ACS Nano*. 2024; 18: 8107-8124.DOI: 10.1021/acsnano.3c11661.

[151] Jie L, Liu H, Hui G, et al. Reduced plasma levels of neuregulin-1 are associated with adverse outcomes in patients with atherosclerotic cardiovascular disease. *Front. Cardiovasc. Med.* 2025; 12: 1600480.DOI: 10.3389/fcvm.2025.1600480.

[152] Hu S, Zhu D, Li Z, et al. Detachable microneedle patches deliver mesenchymal stromal cell factor-loaded nanoparticles for cardiac repair. *ACS Nano*. 2022; 16: 15935-15945.DOI: 10.1021/acsnano.2c03060.

[153] Liang Y, Wang J, Wu X, et al. The prediction value of platelet-derived growth factor for major adverse cardiovascular events in patients with acute non-ST-segment elevation myocardial infarction. *Ann. Med.* 2023; 55: 1047-1057.DOI: 10.1080/07853890.2023.2176542.

[154] Zhang H, Jiang H, Xie W, et al. LNPs-mediated VEGF-C mRNA delivery promotes heart

repair and attenuates inflammation by stimulating lymphangiogenesis post-myocardial infarction. *Biomaterials*. 2025; 322: 123410.DOI: 10.1016/j.biomaterials.2025.123410.

[155] Rufaihah AJ, Johari NA, Vaibavi SR, et al. Dual delivery of VEGF and ANG-1 in ischemic hearts using an injectable hydrogel. *Acta Biomater.* 2017; 48: 58-67.DOI: 10.1016/j.actbio.2016.10.013.

[156] Yuan J, Yang H, Liu C, et al. Microneedle patch loaded with exosomes containing microRNA-29b prevents cardiac fibrosis after myocardial infarction. *Adv. Healthcare Mater.* 2023; 12: 2202959.DOI: 10.1002/adhm.202202959.

[157] Sepehri M, Rabbani S, Ai J, et al. Therapeutic potential of exosomes derived from human endometrial mesenchymal stem cells for heart tissue regeneration after myocardial infarction. *Regener. Ther.* 2025; 28: 451-461.DOI: 10.1016/j.reth.2025.01.007.

[158] Chen Y, Wang R, Cai Y, et al. Dual-tasking PVA-tannic acid-coated ZIF-8/PVDF blended membrane for simultaneous high-flux oil-water emulsion separation and Pb^{2+} adsorption. *J. Hazard. Mater.* 2025; 499: 140282.DOI: 10.1016/j.jhazmat.2025.140282.

[159] García Olloqui P, Rodriguez Madoz JR, Di Scala M, et al. Effect of heart ischemia and administration route on biodistribution and transduction efficiency of AAV9 vectors. *J. Tissue Eng. Regener. Med.* 2020; 14: 123-134.DOI: 10.1002/term.2974.

[160] Shi H, Xue T, Yang Y, et al. Microneedle-mediated gene delivery for the treatment of ischemic myocardial disease. *Sci. Adv.* . 2020; 6: eaaz3621.DOI: 10.1126/sciadv.aaz3621.

[161] Jiang L, Liang J, Huang W, et al. CRISPR activation of endogenous genes reprograms fibroblasts into cardiovascular progenitor cells for myocardial infarction therapy. *Mol. Ther.* 2022; 30: 54-74.DOI: 10.1016/j.ymthe.2021.10.015.

[162] Park H, Kim D, Cho B, et al. In vivo therapeutic genome editing via CRISPR/Cas9

magnetoplexes for myocardial infarction. *Biomaterials*. 2022; 281: 121327.DOI: 10.1016/j.biomaterials.2021.121327.

[163] Wang J, Jiang X, Zhao L, et al. Lineage reprogramming of fibroblasts into induced cardiac progenitor cells by CRISPR/Cas9-based transcriptional activators. *Acta Pharm. Sin. B*. 2020; 10: 313-326.DOI: 10.1016/j.apsb.2019.09.003.

[164] Li L, Lu M, Guo L, et al. An organ-wide spatiotemporal transcriptomic and cellular atlas of the regenerating zebrafish heart. *Nat. Commun.* 2025; 16: 3716.DOI: 10.1038/s41467-025-59070-0.

[165] Chaffin M, Papangeli I, Simonson B, et al. Single-nucleus profiling of human dilated and hypertrophic cardiomyopathy. *Nature*. 2022; 608: 174-180.DOI: 10.1038/s41586-022-04817-8.

[166] Li Y, Li Z, Zhang C, et al. Cardiac fibroblast-specific activating transcription factor 3 protects against heart failure by suppressing MAP2K3-p38 signaling. *Circulation*. 2017; 135: 2041-2057.DOI: 10.1161/CIRCULATIONAHA.116.024599.

[167] Zhang S, Xiang B, Zhao Y, et al. Single-cell epigenomic and transcriptomic analysis unveils the pivotal role of GATA5/ISL1^{+} fibroblasts in cardiac repair post-myocardial infarction. *Cardiovasc. Res.* 2025; 121: 1419-1432.DOI: 10.1093/cvr/cvaf101.

[168] Wang W, Ge T, Chen X, et al. Advances in the protective mechanism of NO, H_2S, and H_2 in myocardial ischemic injury. *Front. Cardiovasc. Med.* 2020; 7: 588206.DOI: 10.3389/fcvm.2020.588206.

[169] Zheng H, Jia F, Gao Y, et al. Injectable protein hydrogel microspheres with reactive oxygen species-responsive nitric oxide release for cardiac protection against ischemia/reperfusion injury. *Acta Biomater.* 2025; 25: 176-192.DOI: 10.1016/j.actbio.2025.08.040.

[170] Wang D, Zhang H, Chen Y, et al. Improving therapeutic effects of exosomes encapsulated gelatin methacryloyl/hyaluronic acid blended and oxygen releasing injectable hydrogel by cardiomyocytes induction and vascularization in rat myocardial infarction model. *Int. J. Biol. Macromol.* 2024; 271: 132412.DOI: 10.1016/j.ijbiomac.2024.132412.

[171] Fan Z, Xu Z, Niu H, et al. An injectable oxygen release system to augment cell survival and promote cardiac repair following myocardial infarction. *Sci. Rep.* 2018; 8: 1371.DOI: 10.1038/s41598-018-19906-w.

[172] Hao T, Ji G, Qian M, et al. Intracellular delivery of nitric oxide enhances the therapeutic efficacy of mesenchymal stem cells for myocardial infarction. *Sci. Adv.* 2023; 9: eadi9967.DOI: 10.1126/sciadv.adi9967.

[173] Hou J, Pan Y, Zhu D, et al. Targeted delivery of nitric oxide via a 'bump-and-hole'-based enzyme-prodrug pair. *Nat. Chem. Biol.* 2019; 15: 151-160.DOI: 10.1038/s41589-018-0190-5.

[174] Benrahla DE, Mohan S, Trickovic M, et al. An orally active carbon monoxide-releasing molecule enhances beneficial gut microbial species to combat obesity in mice. *Redox Biol.* 2024; 72: 103153.DOI: 10.1016/j.redox.2024.103153.

[175] Liu L, Yao Y, Liu Y, et al. Targeted H_2S-mediated gas therapy with pH-sensitive release property for myocardial ischemia-reperfusion injury by platelet membrane. *Biomater. Res.* 2024; 28: 0061.DOI: 10.34133/bmr.0061.

[176] Zhang N, Li T, Zhong P, et al. Design and synthesis of a NTR-sensitive fluorescent H_2S donor as a potential therapeutic agent for myocardial ischemia-reperfusion injury. *J. Med. Chem.* 2025; 68: 14981-14994.DOI: 10.1021/acs.jmedchem.5c01169.

[177] Zhu D, Hou J, Qian M, et al. Nitrate-functionalized patch confers cardioprotection and improves heart repair after myocardial infarction via local nitric oxide delivery. *Nat. Commun.*

2021; 12: 4501.DOI: 10.1038/s41467-021-24804-3.

[178] Hao T, Qian M, Zhang Y, et al. An injectable dual-function hydrogel protects against myocardial ischemia/reperfusion injury by modulating ROS/NO disequilibrium. *Adv. Sci.* . 2022; 9: 2105408.DOI: 10.1002/advs.202105408.

[179] Zhang Y, Yu W, Zhang L, et al. Nanozyme-based visual diagnosis and therapeutics for myocardial infarction: the application and strategy. *J. Adv. Res.* 2025; 70: 187-201.DOI: 10.1016/j.jare.2024.04.019.

[180] Wang Y, Duan X, Men C, et al. Multifunctional microneedle patch loaded with microfluidic-synthesized hybrid gas-nanozyme for myocardial infarction treatment. *J. Nanobiotechnol.* 2026; 24: 65.DOI: 10.1186/s12951-025-03920-y.

[181] Wang Q, Cao S, Zhang T, et al. Reactive oxide species and ultrasound dual-responsive bilayer microneedle array for in-situ sequential therapy of acute myocardial infarction. *Biomater. Adv.* 2024; 162: 213917.DOI: 10.1016/j.bioadv.2024.213917.

[182] Chen Y, Mu Z, Hu Y, et al. Porous microneedles delivering apoptotic body-camouflaged nanozymes promote diabetic wound repairment through combined pro-angiogenesis, anti-inflammation, and bacterial elimination. *Colloids Surf., B*. 2025; 114966.DOI: 10.1016/j.colsurfb.2025.114966.

[183] Gu Z, Liu X, Qi Z, et al. An antioxidant nanozyme for targeted cardiac fibrosis therapy post myocardial infarction. *J. Nanobiotechnol.* 2024; 22: 760.DOI: 10.1186/s12951-024-03047-6

[184] Liu S, Xin R, Zhang X, et al. Separable microneedle patch integrated with the dictamnine-loaded copper MOF nanozyme for atopic dermatitis treatment. *ACS Appl. Mater. Interfaces*. 2025; 17: 26386-26401.DOI: 10.1021/acsami.5c02334.

[185] Li Z, Wu B, Li W, et al. Unlocking an efficient SOD-to-CAT catalytic relay in a MOF

nanozyme via dopamine-driven interfacial nanoreconstruction for osteoarthritis therapy. *Adv. Mater.* 2026; 38: e72747.DOI: 10.1002/adma.72747.

Table 1. Pathological stage-matched design of hydrogel MNs for MI repair.

MI stage	Pathological features	Targeted MN functionalities	Representative therapeutic agents
Acute injury (0-24 h)	Cardiomyocyte necrosis, ROS burst	ROS scavenging, oxygen delivery, anti-apoptosis	Antioxidant nanozymes
Inflammatory phase (1-7 d)	Immune cell infiltration, cytokine storm	Immunomodulation, anti-inflammation,	Anti-inflammatory cytokines, macrophage-polarizing agents
Proliferative/ repair phase (7-21 d)	Angiogenesis, fibroblast activation	Pro-angiogenesis, growth factor delivery, ECM support	VEGF, bFGF, exosomes, pro-repair miRNAs
Remodeling/ scar formation (>21 d)	Fibrosis, scar maturation, ventricular wall thinning	Anti-fibrosis, mechanical support	Anti-fibrotic drugs, ECM-crosslinking agents

Table 2. Comparative analysis of drug delivery strategies for MI.

Parameter	Intramyocardial Injection	Conventional Hydrogel Patch	Nanoparticle-based Delivery	Hydrogel MN Patch
Invasiveness	High (open chest/needle puncture)	Moderate (epicardial placement)	Low (systemic injection or catheter)	Low-Moderate (epicardial placement)
Spatial targeting	Poor (single point, bolus diffusion)	Moderate (surface contact, passive diffusion)	Poor (systemic off-target)/Good (if targeted)	High (direct penetration into infarct/border zone)
Drug release kinetics	Burst release, short half-life	Sustained, diffusion-controlled	Tunable (controlled release possible)	Sustained, spatially graded (multiple layers possible)
Tissue retention	Poor (washout due to beating heart)	Moderate (adhesion-dependent)	Poor (systemic clearance)	Good (mechanical anchoring)
Foreign body /safety concerns	Low (single injection)	Moderate (patch may dislodge)	Low-Moderate (depending on material)	Moderate-High (penetrating foreign body, potential arrhythmia)
Clinical translation status	Established (cell/gene therapy trials)	Early clinical (alginate patches)	Established (liposomal doxorubicin)	Preclinical (proof-of-concept)
Key limitation	Drug washout, uneven distribution	Poor penetration into myocardium	Systemic off-target effects, low cardiac accumulation	Manufacturing complexity, long-term foreign body response

Table 3. Summary of microneedle design parameters for HFM development.

Parameter	Size and dimension
Length of needle (L)	600 µm [64,73-76]
	700 µm [77]
	800 µm [78]
	1000 µm [79]
Diameter of needle base (Db)	150 µm [80]
	250 µm [77]
	410 µm [78]
Tip diameter (*D*t)	<15 µm [70]
Array size (*Ax* vs *Ay*)	1×9 [80]
	10×10 [81]
	11×11 [78]
	15×15 [79]

Table 4. Comparative analysis of microneedle fabrication methods for cardiac applications.

Parameter	Micro-molding	3D Printing
Scalability	High; amenable to roll to roll manufacturing	Low to moderate; batch processing, limited by print speed and build volume
Reproducibility	High once master mold is fabricated; low batch to batch variability	Moderate; depends on printer calibration, resin batch, and environmental conditions
Cost	Low per unit at large scale; high initial tooling cost for master mold	High per unit; equipment and resin/maintenance costs significant
Manufacturing constraints	Limited to thermoset or UV-curable polymers; demolding challenges for high aspect ratio MNs	Design flexibility high; but resolution throughput trade-off; post-processing (washing, post-cure) required
Clinical translation suitability	Favorable for mass production of disposable patches; established regulatory pathways for similar medical devices	Emerging; suitable for patient-specific or personalized patches; but quality assurance and sterilization remain challenges
Material compatibility	Broad	Dependent on resin photocurability; limited for some biodegradable materials
Resolution	High (replicates master mold features down to ~1 µm)	Very high for TPP (sub-µm); lower for extrusion (~100 µm)

Table 5. Clinical translation bottlenecks for hydrogel microneedles in MI therapy: challenges and proposed solutions.

Bottleneck	Key Challenge	Proposed Solution(s)
Delivery precision	Accurate insertion under beating-heart conditions without damaging vessels or perforating ventricle	Real-time imaging guidance
Scalability & GMP	Lab-scale, batch-variable, non-sterile production	Continuous manufacturing
Long-term safety	Unknown fate of degradation products; potential chronic inflammation or arrhythmia	Benign, renally clearable polymers
Regulatory pathway	Unclear classification as combination product	Stepwise de-risking framework

Table 6. Comparison between synthetic and natural materials.

	Synthetic materials	Natural materials
Advantages	Adjustable mechanical properties, lower batch to batch variability, and easier standardization and storage	Generally better biocompatibility and biodegradability, and retention of natural microstructure and biological properties
Disadvantages	Inferior biocompatibility and biodegradability, lack of natural cell adhesion sites, and degradation products may cause adverse reactions (infection and calcification)	Weaker mechanical properties, higher batch to batch variability, and greater difficulty in standardization and storage
Prevalent use in cardiac patches	PCL, PU, PEG, PVA, PGS, PNIPAAm, PLCA, and PLGA	Fibrin, collagen, gelatin, dECM, silk fibroin, chitosan, HA, and alginates

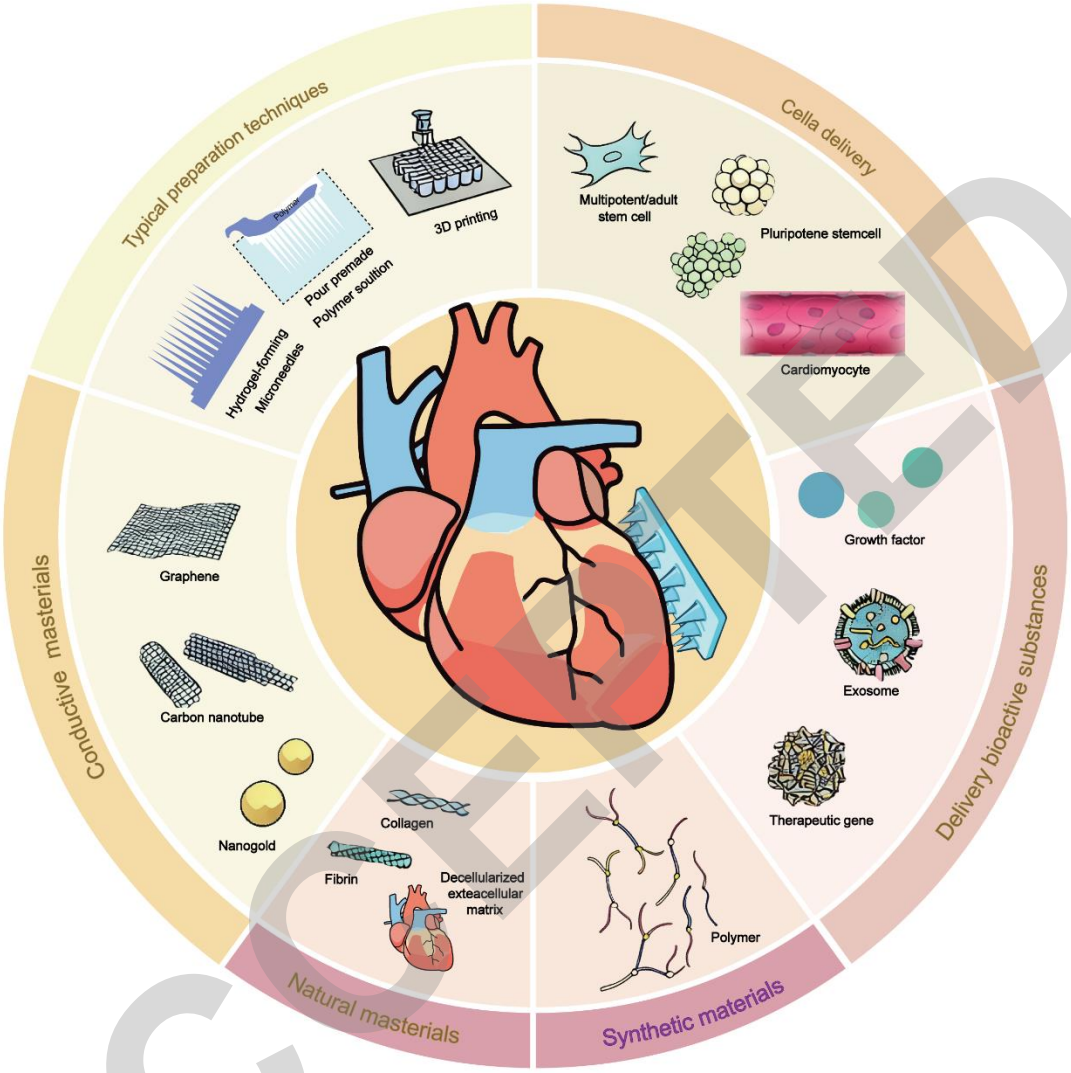

Figure 1. Schematic summary of hydrogel MNs for MI treatment.

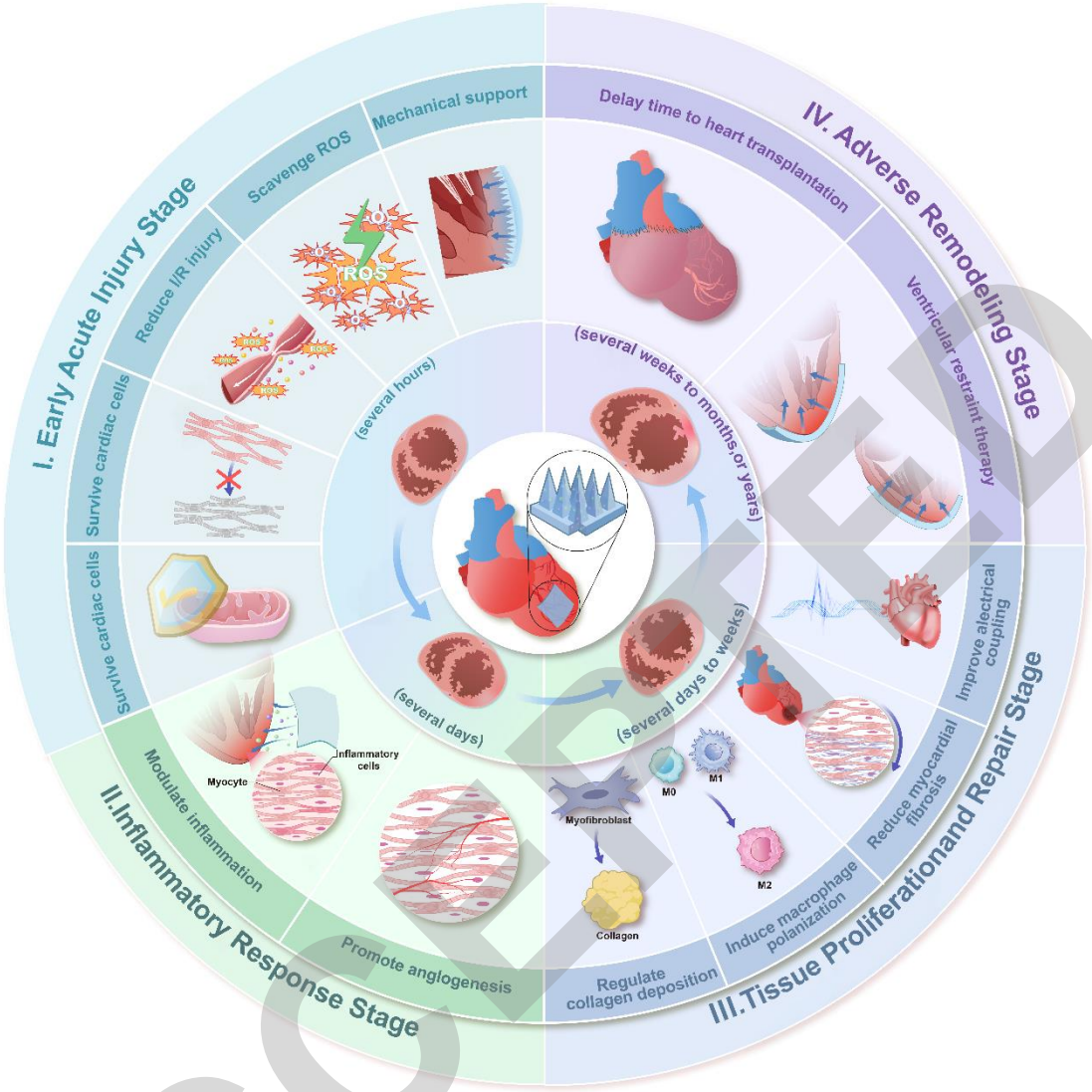

Figure 2. Schematic overview of sequential stages in the progression of myocardial infarction and corresponding therapeutic interventions via hydrogel MNs.

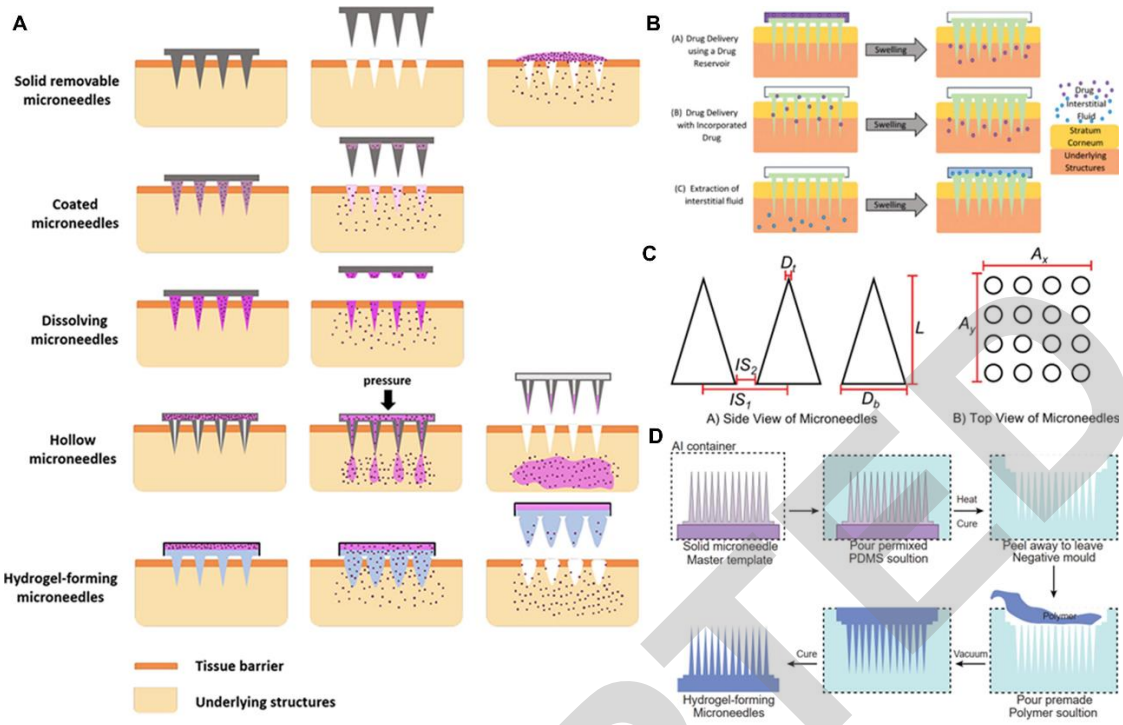

Figure 3. Classification of MNs, drug delivery strategies, MNs design, and preparation methods for hydrogel MNs. (A) From types to application: a schematic illustrating microneedle classification and their mechanisms for trans-tissue drug delivery. [63] Copyright 2018, Elsevier. (B) Schematic to show the different mechanisms of hydrogel MNs for drug delivery. [86] Copyright 2021 The Joseph G. Turners. (C) Schematic diagrams showing the different dimensions taken into consideration for microneedle arrays. Showing (a) side view of microneedles and (b) top view of microneedle array. Where: IS—Interneedle spacing, *D*—Diameter, *L*—Length, *A*—Array. [86] Copyright 2021 The Joseph G. Turners. (D) Schematic to show the micro-molding method for the production of hydrogel MNs. [86] Copyright 2021 The Joseph G. Turners.

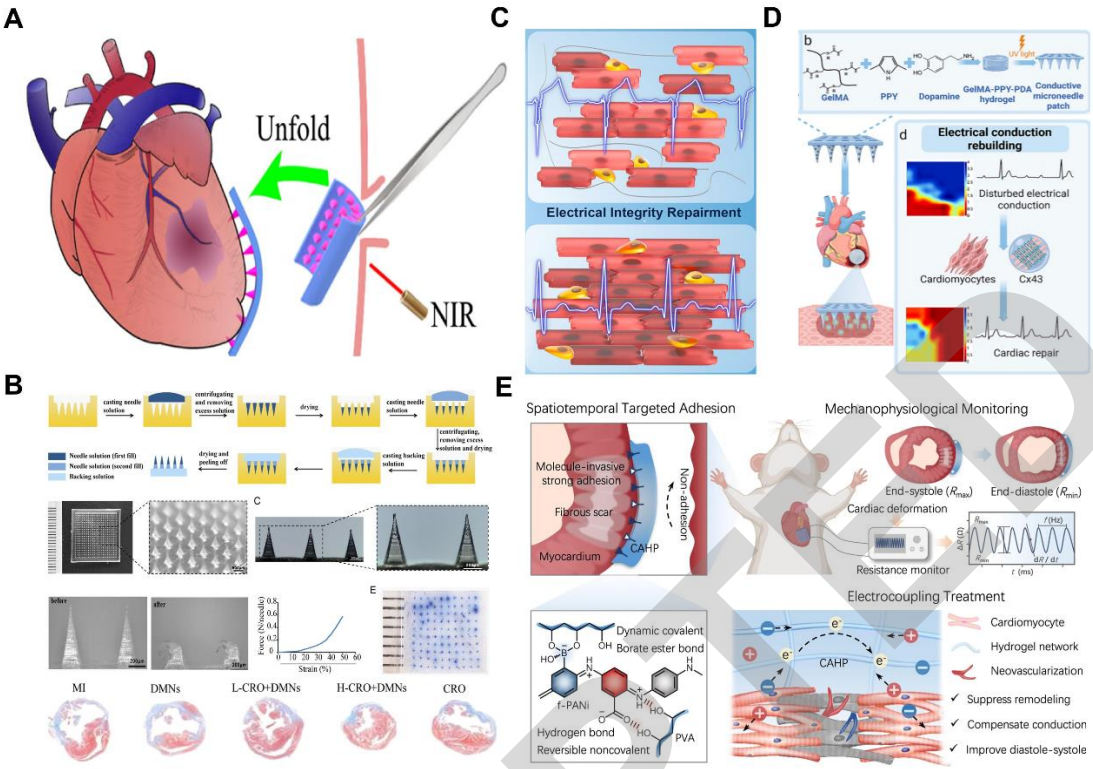

Figure 4. Application of synthetic, natural, and conductive material-derived patches in the treatment of MI. (A) Schematic of the overall treatment design of treating MI with GO-PVA MN. [96] Copyright 2021, American Chemical Society. (B) Preparation and characterization of DMNs. Masson's trichrome stained images of heart sections from each group at 28 d after MI. [46] Copyright 2025, The Qian Lius. (C) Schematic illustration of the electrocoupling treatment for MI with conductive patches, capable of bridging the infarct area to improve electrical conduction. [123] Copyright 2024, Elsevier. (D) Scheme of fabrication of conductive microneedle and electrical reconnection mechanism by conductive microneedles in infarcted myocardium, thereby promoting cardiac repair. [55] Copyright 2025, The Yi-an Maos. (E) Chronological tissue adhesion was enabled by dynamic covalent/noncovalent interfaces between functionalized

polyaniline and PVA, achieving strong, molecule-invasive myocardial bonding while preventing off-target adhesion. [111] Copyright 2023, The Chaojie Yus.

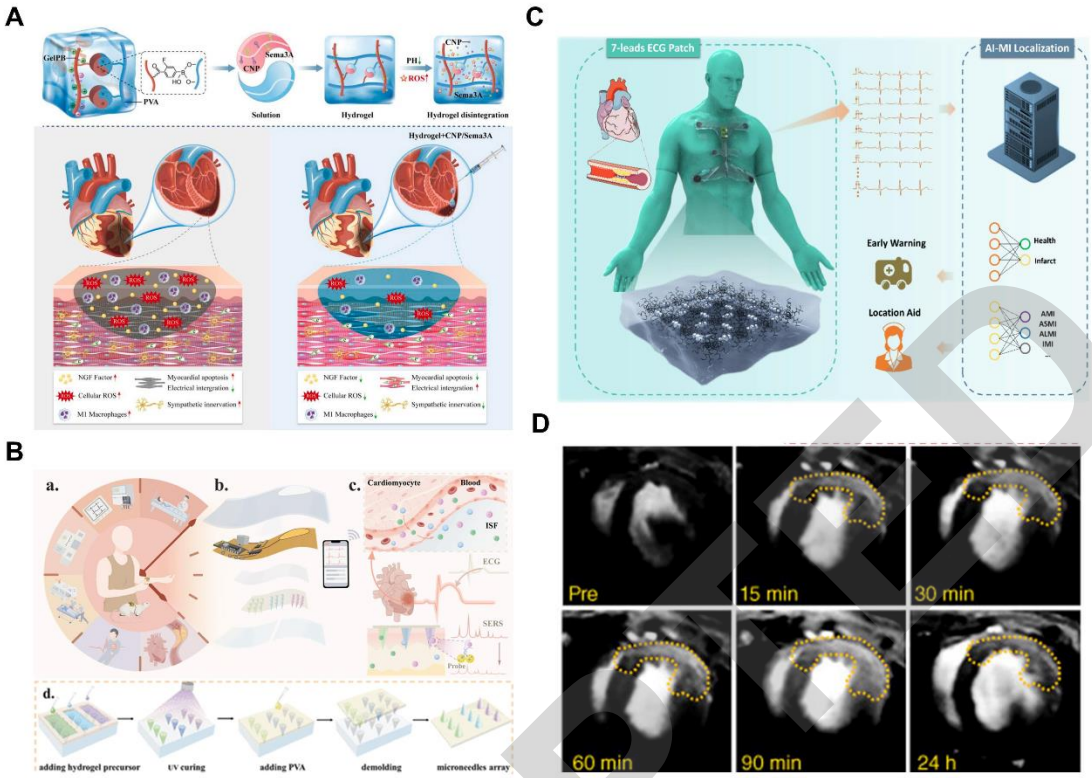

Figure 5. Smart responsive, monitoring, magnetic resonance imaging in the treatment of MI. (A) Schematic of the preparation process and mechanism of action of an injectable hydrogel co-loaded with CNP and Sema3a for sympatho-immune regulation post MI. [10] Copyright 2025, Elsevier. (B) Schematic representation of the detection principle of the e-SERS patch. [138] Copyright 2025, American Chemical Society. (C) Concept display of soft heart monitoring patches for MI prevention and localization, equipped with homemade SCL bioelectrodes. [139] Copyright 2025, American Chemical Society. (D) Representative in vivo MRI of ischemia-reperfusion (I/R) heart before and during the first 24 h post the administration of GCD/Qt@ZIF-RGD by tail vein injection. Yellow circles indicate the hyper-enhancement of the infarcted myocardium. [140] Copyright 2024, Taylor & Francis.

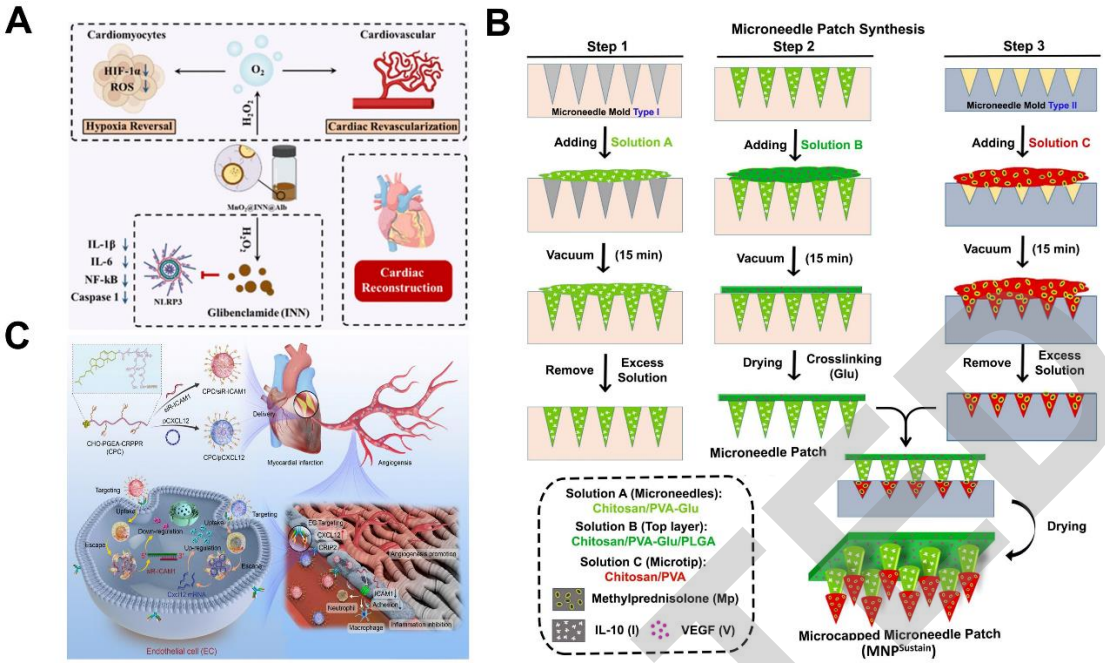

Figure 6. Functionalization drug delivery strategies such as single drug, sequential therapy, and combination therapy in the treatment of MI. (A) Ameliorating MI by concurrent proptosis suppression and on-demand oxygen production via functionalized nanocarrier. [146] Copyright 2025, The Wenwu Zhus. (B) Fabrication of $MNP^{Sustain}$. [45] Copyright 2025, Elsevier. (C) A schematic representation depicting the assembly of CPC/siR-ICAM1 and CPC/pCXCL12 complexes, as well as a targeted combination therapy for cardiac endothelium aimed at treating MI. [150] Copyright 2024, American Chemical Society.

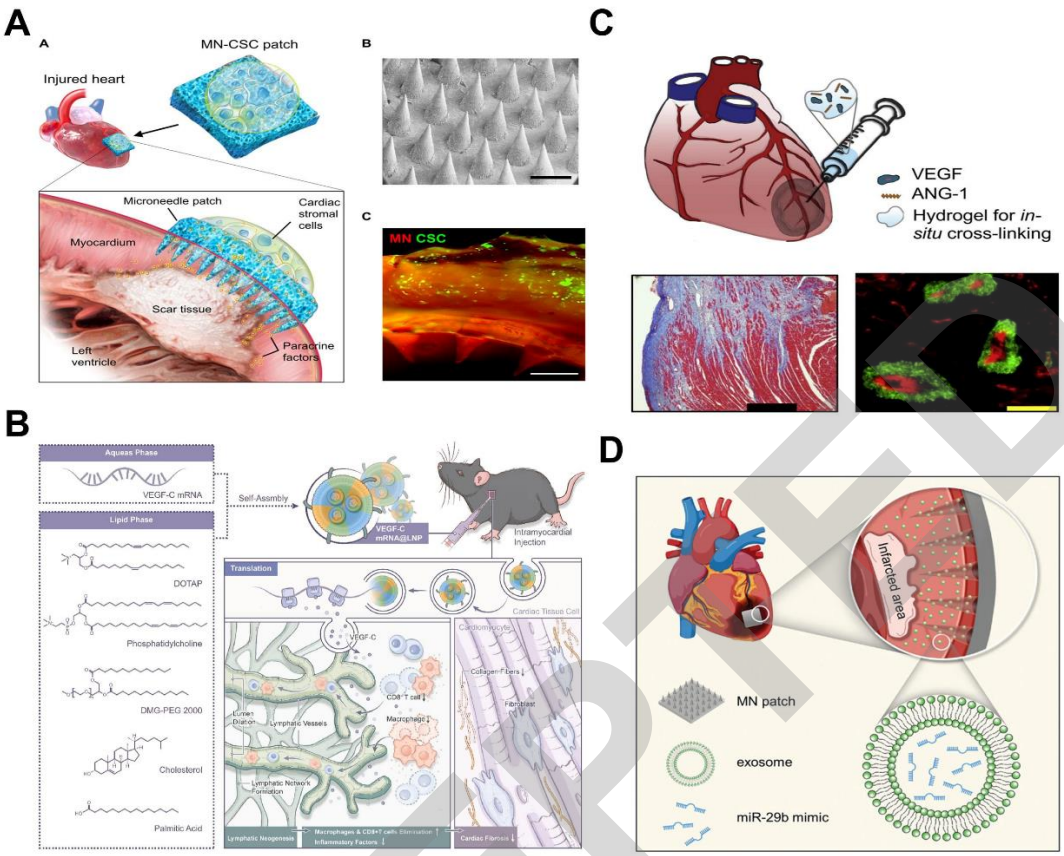

Figure 7. Cell therapy, growth factors, exosomes in the treatment of MI. (A) Schematic of the experimental design for evaluating MN-CSC therapy in infarcted hearts; SEM image of the microneedle (MN) array; and a representative fluorescent micrograph showing DiO-labeled CSCs (green) encapsulated in fibrin gel and integrated onto the MN array (red). [131] Copyright 2018, The Junnan Tangs. (B) A lipid nanoparticle loaded with VEGF-C mRNA was designed for the treatment of MI. [154] Copyright 2025, Elsevier. (C). Schematic diagram of PF hydrogel for sustained dual delivery of VEGF and ANG-1 to enhance myocardial repair and function. [155] Copyright 2017, Elsevier. (D) Schematic illustration of the MN patch loaded with exosomes containing miR-29b mimics for MI treatment. [156] Copyright 2023, Wiley-VCH GmbH.

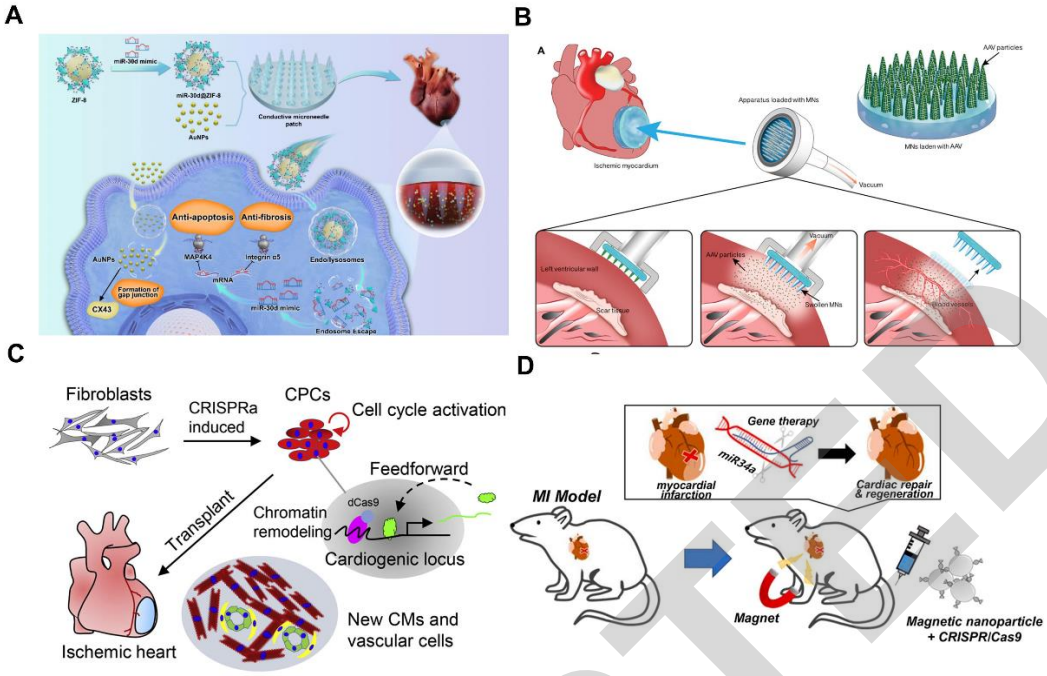

Figure 8. Gene therapy strategies in the treatment of MI. (A) Integration of a conductive microneedle patch and a miR-30d delivery system alleviated myocardial ischemia–reperfusion injury. [117] Copyright 2024, American Chemical Society. (B) Ischemic hearts received MN-AAV through a specially designed device. [160] Copyright 2020, The Hongpeng Shis. (C) The endogenous genes Gata4, Nkx2.5, and Tbx5 could be rapidly activated in adult cardiac fibroblasts in vitro through the CRISPR activation system, thereby establishing autonomous regulatory circuits and initiating the formation of CPCs for the treatment of ischemic MI. [161] Copyright 2022, Elsevier. (D) Schematic representation of the delivery system developed using Cas9 magnetoplexes. [162] Copyright 2022, Elsevier.

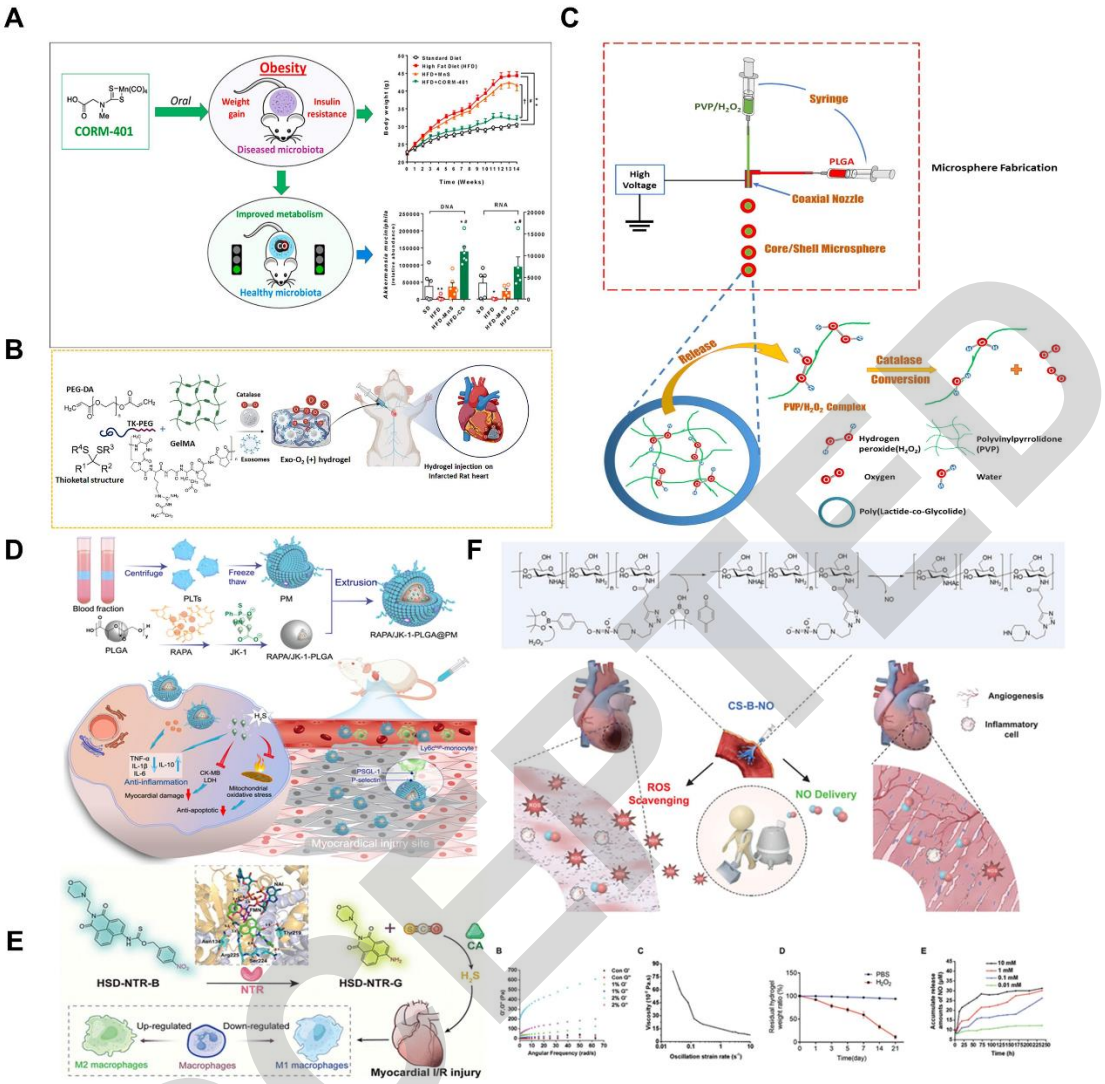

Figure 9. Gas therapies such as CO, O_2, H_2S, and NO in the treatment of MI. (A) Schematic diagram of CO therapy for MI and CO release. [174] Copyright 2024, Elsevier. (B) Schematic depicting the preparation of an injectable, oxygen-generating hydrogel for acute myocardial therapy, based on a blended GelMA and TK-PEG matrix loaded with catalase and exosomes. [170] Copyright 2024, Elsevier. (C) Fabrication oxygen release microsphere and oxygen release mechanism. [171] Copyright 2018, The Zhaobo Fans. (D) Schematic of nanoparticles designed for MI targeting, pH-responsive drug release, and the co-delivery of JK-1 and RAPA toward gas

therapy. [175] Copyright 2024, The Lin Lius. (E) Schematic illustration of HSD-NTR-B for the treatment of MI. [176] Copyright 2025, American Chemical Society. (F) Illustration outlining the approach to addressing I/R heart damage using CS-B-NO, along with the characterization of an injectable chitosan hydrogel that possesses a ROS-responsive function for releasing NO. [178] Copyright 2022, The Tian Haos.

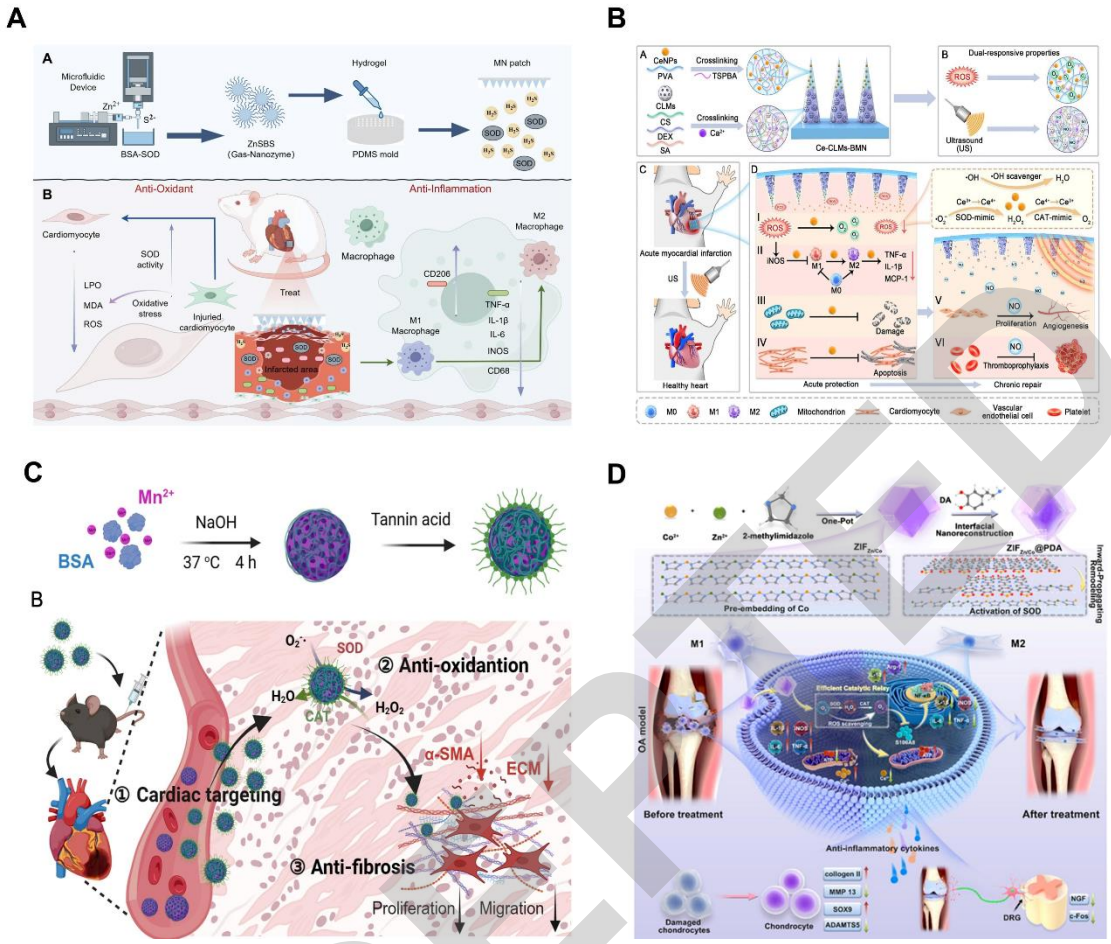

Figure 10. Nano-enzyme for the treatment of myocardial infarction and other applications. (A) Schematic illustration of preparation and therapeutic mechanism of Gas-nanozyme MN patches. Preparation of hybrid gas-nanozyme via a microfluidic method. MN patches sustainably release H_2S to reduce oxidative stress and regulate inflammation for MI treatment. [180] Copyright 2024, Springer Nature. (B) The construction of Ce-CLMs-BMN and its application in treating AMI. [181] Copyright 2024, Elsevier. (C) Schematic illustration of preparation of tannin acid-modified nanozyme (named as MnO_2@TA) and application for the treatment of MI by cardiac-targeted anti-oxidation and anti-fibrosis. [183] Copyright 2024, The Ziyi Gus. (D) Schematic illustration of the preparation process of $ZIF_{Zn/Co}$@PDA nanozymes and their

therapeutic effect on osteoarthritis and the nanozymes with SOD-CAT activity were synthesized through nanoscale interface reconstruction of DA on Zn/Co-based MOF nanoparticles. [185]